Solar Physics (2005) 225: 105–139

CORONAL SHOCKS OF NOVEMBER 1997 REVISITED: THE CME–TYPE II TIMING PROBLEM

E. W. CLIVER[1], N. V. NITTA,[2] B. J. THOMPSON[3] and J. ZHANG[4]
[1]*Air Force Research Laboratory, Space Vehicles Directorate, Hanscom AFB, MA 01731-3010, USA (e-mail: edward.cliver@hanscom.af.mil)*
[2]*Lockheed Martin Solar and Astrophysics Laboratory, O/L9-41, B/252, 3251 Hanover Street, Palo Alto, CA 94304, USA (e-mail: nitta@lmsal.com)*
[3]*NASA Goddard Space Flight Center, Code 682.3, Greenbelt, MD 20771, USA (e-mail: barbara.j.thompson@nasa.gov)*
[4]*Center for Earth Observing and Space Research, George Mason University, Fairfax, VA 22030, USA (e-mail: jiez@scs.gmu.edu)*

(Received 11 May 2004; accepted 24 August 2004)

Abstract. We re-examine observations bearing on the origin of metric type II bursts for six impulsive solar events in November 1997. Previous analyses of these events indicated that the metric type IIs were due to flares (either blast waves or ejecta). Our point of departure was the study of Zhang *et al.* (2001) based on the Large Angle and Spectrometric Coronagraph's C1 instrument (occulting disk at 1.1 R_0) that identified the rapid acceleration phase of coronal mass ejections (CMEs) with the rise phase of soft X-ray light curves of associated flares. We find that the inferred onset of rapid CME acceleration in each of the six cases occurred 1–3 min before the onset of metric type II emission, in contrast to the results of previous studies for certain of these events that obtained CME launch times ~25–45 min earlier than type II onset. The removal of the CME-metric type II timing discrepancy in these events and, more generally, the identification of the onset of the rapid acceleration phase of CMEs with the flare impulsive phase undercuts a significant argument against CMEs as metric type II shock drivers. In general, the six events exhibited: (1) ample evidence of dynamic behavior [soft X-ray ejecta, extreme ultra-violet imaging telescope (EIT) dimming onsets, and wave initiation (observed variously in Hα, EUV, and soft X-rays)] during the inferred fast acceleration phases of the CMEs, consistent with the cataclysmic disruption of the low solar atmosphere one would expect to be associated with a CME; and (2) an organic relationship between EIT dimmings (generally taken to be source regions of CMEs) and EIT waves (which are highly associated with metric type II bursts) indicative of a CME-driver scenario. Our analysis indicates that the broad (~90° to halo) CMEs observed in the outer LASCO coronagraphs for these impulsive events began life as relatively small-scale structures, with angular spans of ~15° in the low corona. A review of on-going work bearing on other aspects (than timing) of the question of the origin of metric type II bursts (CME association; connectivity of metric and decametric-hectometric type II shocks; spatial relationship between CMEs and metric shocks) leads to the conclusion that CMEs remain a strong candidate to be the principal/sole driver of metric type II shocks vis-à-vis flare blast waves/ejecta.

1. Introduction

Solar metric type II bursts (reviewed by Nelson and Melrose, 1985) drift outward through the low corona from high to low frequencies at rates ~0.5 MHz s^{-1}, corresponding to speeds of ~500–1000 km s^{-1}. These "slow-drift" bursts are attributed to shock accelerated electrons that excite plasma waves that convert into escaping

radio waves. The origin of metric type II bursts has been a matter of controversy, with the two candidate sources being solar flares (either flare blast waves caused by a sudden short-range expansion of the flare volume caused by impulsive heating (Parker, 1961; Uchida, 1974a,b; Vršnak and Lulić, 2000a,b; Hudson *et al.*, 2003) or flare ejecta (Giovanelli and Roberts, 1958; Gopalswamy *et al.*, 1997, 1999a; Klein *et al.*, 1999)) and coronal mass ejections (CMEs) (Gosling *et al.*, 1976; Maxwell, Dryer, and McIntosh, 1985; Cliver, Webb, and Howard, 1999; Mancuso *et al.*, 2004). At present, it is not known which, if either, of these sources is dominant (e.g., Classen and Aurass, 2002).

One of the strongest arguments for the flare blast wave scenario for metric type IIs is the close timing between flares and type II onset (Kundu, 1965; Vršnak *et al.*, 1995), with type IIs typically beginning within a few minutes of the impulsive phase of the flare. In contrast, there are events for which reported CME launch times occur well in advance (>20 min) of associated type II bursts (Leblanc *et al.*, 2000). These CME–type II timing results were based on extrapolation of CME height-time plots from data taken by the Large Angle and Spectrometric Coronagraph's (LASCO) (Brueckner *et al.*, 1995) C2 and C3 instruments on the Solar and Heliospheric Observatory (SOHO) with fields of view from 2–6 R_0 and 4–30 R_0, respectively. Specific cases showing lack of close timing agreement between type IIs and CMEs are in accord with a general perception (e.g., Kahler, 1992; Gosling, 1993; Harrison, 1995) that only a loose temporal/spatial relationship exists between flares and CMEs.

Recently, Zhang *et al.* (2001) used the LASCO C1 instrument (field of view from 1.1–3 R_0) and the EUV imaging telescope (EIT) (Delaboudinière *et al.*, 1995), which observes the solar disk and the corona up to 1.5 R_0, to determine CME launch times without any need for extrapolations and their attendant uncertainties. For four well-observed limb or near limb events (60–92° in longitude from solar central meridian), Zhang *et al.* found that CME launch typically consists of a slow-rising (<80 km s^{-1}) initiation phase followed by an impulsive acceleration (100–500 m s^{-2}) phase, although for an impulsive X9 soft X-ray event on 6 November 1997, the CME lacked an initiation phase and exhibited an extreme acceleration rate of 7300 m s^{-2}. Zhang *et al.* found that the CME height above the limb at the onset of the impulsive acceleration phase ranged from ~1.35–1.5 R_0 and that the impulsive acceleration phase coincided with the rise phase of the main flare event in the soft X-ray light curve (following any preflare (precursor)/CME initiation phase that might have occurred). From a study of three events using LASCO and EIT data, Neupert *et al.* (2001) similarly noted that the CME explosive phase onset coincided with an abrupt increase in flare soft X-ray emission. Additional examples (not all independent) of events exhibiting this behavior can be found in the work of Kahler *et al.* (1998), Alexander, Metcalf, and Nitta (2002), Yurchyshyn (2002), Gallagher, Lawrence, and Dennis (2003), Shanmugaraju *et al.* (2003), Subramanian *et al.* (2003), Wang *et al.* (2003), Zhang *et al.* (2004), Qui *et al.* (2004), and Kundu *et al.* (2004). While the details of the relationship between

flare development and CME acceleration may vary somewhat from event to event (e.g., Kundu *et al.*, 2004), the basic picture of a close link between the flare impulsive phase and the rapid phase of CME acceleration seems well established. Thus the soft X-ray time profile provides a useful means of inferring CME dynamics in the low corona (particularly since the C1 coronagraph ceased operation in June 1998) that we will exploit in this study.

In Section 2, we investigate the relationship between the CME rapid acceleration phase and type II onset for six events occurring in November 1997 that have figured prominently in the debate on the "flare vs. CME" origin of metric type II bursts. Each of these events has been investigated by one or more sets of authors with the general conclusion that flare blast waves or flare ejecta were responsible for the metric type II emission. In this study, using the Zhang *et al.* (2001) study as a point of departure and focusing on *Yohkoh* soft X-ray telescope (SXT; Tsuneta *et al.*, 1991) and EIT images (and C1 data when available), we re-examine the CME–type II timing relationship for these reported examples of flare origin events and conclude that the data are consistent with the CME-driver scenario. In Section 3, we review other lines of on-going research that bear on the origin of metric type II shocks. Results are summarized in Section 4 and discussed in Section 5.

2. Timing Analysis

Table I gives a list of the six events with location and timing information, observed flaring region dynamics (from this and other studies as discussed later), and references. Note that the first five of these events (including the 6 November 1997 event analyzed by Zhang *et al.*, 2001) originated in the same active region, NOAA/USAF 8100.[1] All six of the associated flares, ranging in size from C8–X9 in the GOES 1–8 Å classification, were impulsive, with soft X-ray rise phases (excluding precursors) of 3–5 min and durations (at 0.1 of peak intensity) less than 30 min. CMEs were not observed in the C1 coronagraph for the first four flares which were all located within 35° in longitude from disk center.

2.1. 03 NOVEMBER 1997, 04:37 UT

This event has been studied by Reiner and Kaiser (1999), Leblanc *et al.* (2000, 2001), and Narukage *et al.* (2002). The GOES soft X-ray curve for the C8/SB flare and the C2 and C3 height–time data for the CME leading edge are shown in Figure 1. The positions of the data points on the height–time plot for this and the following events were determined by Chris St. Cyr (personal communication, 2004). In the figure, the onset time of the metric type II burst is indicated (placed at

[1] A very similar sequence of impulsive flares from an active region in November 2000 was reported by Nitta and Hudson (2001). Like the Table I events, the November 2000 flares were associated with type II bursts and broad CMEs.

TABLE I

Timings and source locations of the metric type II bursts with associated dynamic phenomena.

	Hα flare		1–8 Å soft X-ray[a]			Metric II[b] onset (UT) S/F (MHz) S/H (km)	CME[c] Speed/width km s^{-1}/°	SXR ejecta	Waves[d]			EIT Dimming[g]	References[h]
Date	Location (Region)	Cl	Cl	Duration (min)	Rise time (UT)				Hα[e]	EIT[f]	SXR		
3 November 97	S20W13	SB	C8	25	0434–0439	0437	227/109	–	1.1×10^5	Q0	√	D5	1–4
	(8100)					130			0436	0502	0435	0502	
						$2.0 \pm 1.0 \times 10^5$							
3 November 97	S18W16	1B	M1	10	0907–0911	0909	658?[i]/?	–	$\sim 1 \times 10^5$	Q3	√	D6	5–7
	(8100)					210			0909	0911	0910	0911	
						$9 \pm 7 \times 10^4$							
3 November 97	S17W22	1N	M4	20	1026–1030	1028?	352/122	–	–	Q3	–	D2	2, 3, 5, 8
	(8100)					120?				1032		1032	
						$2.2 \pm 1.0 \times 10^5$?							
4 November 97	S14W34	3B	X2	15	0556–0559	0558	785/H	?	1.2×10^5	Q1	–	D4	3, 9, 10
	(8100)					115			0558	0614		0614	
						$2.3 \pm 1.1 \times 10^5$							
6 November 97	S18W63	2B	X9	20	1152–1156	1153?	1556/H	?	–	Q2	–	D6	3, 5
	(8100)					250?				1159		1159	11–13
						$7 \pm 6 \times 10^4$							
27 November 97	N16E63	2B	X2	10	1313–1318	1316	441/91	√	–	Q1	–	D4	3, 5, 14
	(8113)					250				1337		1337	
						$7 \pm 6 \times 10^4$							

Notes:

[a]Duration at 0.1 of the peak intensity.

[b]Sources of metric records for type II onsets and starting frequency: 3 November 1997, 0437 UT (Culgoora, Leblanc *et al.*, 2000); 3 November 1997, 0909 UT (Potsdam, Khan and Aurass, 2002); 3 November 1997, 1028 UT (Izmiran, *http://helios.izmiran.rssi.ru/lars/LARS.html*); 4 November 1997, 0558 UT (Culgoora, Dulk *et al.*, 1999); 6 November 1997, 1153 UT (Potsdam, Henry Aurass, personal communication, 2001); 27 November 1997, 1316 UT (Potsdam, Klein *et al.*, 1999). Several of the starting fundamental frequencies were determined by dividing the starting harmonic frequency by two. The records for the events on 3 November, 1028 UT and 6 November, 1153 UT were particularly complex and difficult to interpret.

[c]Taken from SOHO LASCO CME Catalog (http://cdaw.gsfc.nasa.gov/CME_list/), linear fit.

[d]The first time at which the various waves were observed is given in the second row in each column.

[e]The distance in km of the Hα wave from the flaring region is given in the first row.

[f]EIT wave classification (quality rating) from Biesecker *et al.* (2002): Q0 (not likely to be a wave/poor data coverage; <10% confidence level); Q1 (faint appearance / still unclear; <25%); Q2 (propagation of brightened front; >25%); Q3 (propagation of brightened front; >50%); Q4 (almost definitely; >75%); Q6 (clear propagation of front; ~100%).

[g]EIT dimming classification (West and Thompson, 2003): D0 (no dimming was observed with the wave); D1 (dimming is observed, but no apparent spatial correlation with the wave location); D2 (slight overlap between wave trajectory and dimming location); D3 (partial overlap); D4 (dimming between wave and source region, but not perfect overlap); D5 (there is dimming everywhere between the wavefront and the active region); D6 (dimming and wave are co-located, and seen to expand together in multiple images (both temporal and spatial correlation)). The first time at which the dimmings were observed is given.

[h]References: (1) Reiner and Kaiser (1999); (2) Leblanc *et al.* (2000); (3) Leblanc *et al.* (2001); (4) Narukage *et al.* (2002); (5) Klassen *et al.* (2000); (6) Warmuth *et al.* (2001); (7) Khan and Aurass (2002); (8) Reiner *et al.* (2001); (9) Dulk *et al.* (1999); (10) Eto *et al.* (2002); (11) Maia *et al.* (1999); (12) Zhang *et al.* (2001); (13) Cliver *et al.* (2001); (14) Klein *et al.* (1999).

[i]Based on two data points (S. Yashiro, personal communication, 2004). Delannée *et al.* (2000) also report a CME for this event, giving its time of first observation as 1111 UT, versus 0953 UT from Yashiro.

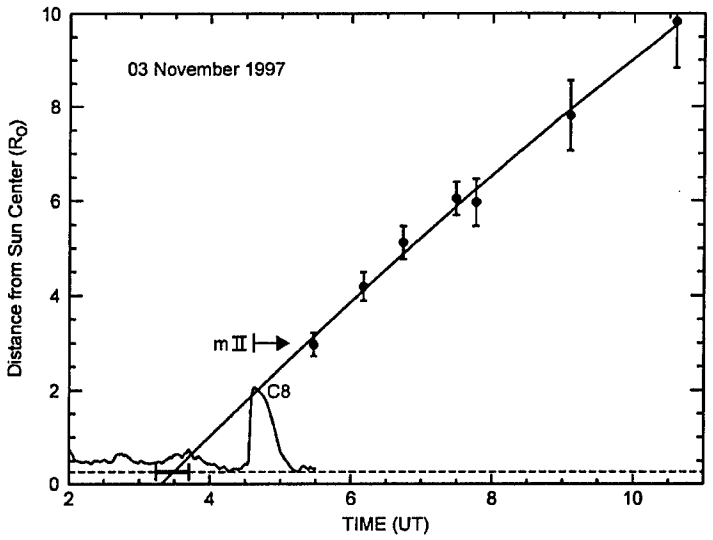

Figure 1. Height–time data for the leading edge of the CME (measured in the plane of the sky) on 3 November 1997 associated with the SB flare (S20W13) at ~0430 UT from NOAA/USAF region 8100. The solid line fitted represents a constant deceleration fit to the LASCO C2 and C3 data points. The dashed horizontal line is drawn at the projected distance of the flare from disk center. Heavy bars on this line reflect uncertainties in the lift-off time of the CME. The GOES 1–8 Å data are plotted and the onset time of the metric type II is indicated. The distance of the type II arrow from the time axis does not correspond to the starting height of the type II; in this and subsequent figures it is placed at an arbitrary height (the nominal height range of metric type II bursts is ~1.1–2.5 R_0).

an arbitrary height, see caption). Leblanc *et al.* (2000, 2001) used a second-order (constant deceleration) fit (not shown) to the C2 and C3 coronagraph data to obtain a CME lift-off time at the flare site (S20W13) of 0412 UT, ~25 min before the metric type II burst onset at 0437 UT. Similarly, Reiner and Kaiser (1999) extrapolated a frequency-time plot of type II emission observed by the Wind/WAVES experiment (Bougeret *et al.*, 1995) in the decametric-hectometric range (14–1 MHz; DH) back in time to obtain a DH type II exciter lift-off time of 0406 UT. Both Reiner and Kaiser (1999) and Leblanc *et al.* (2000, 2001) attributed the DH type II to the observed CME and concluded that the metric type II shock in this event was a flare blast wave – based on the apparent separation between CME launch and metric II onset and the close timing relationship between the flare and the type II burst (Figure 1).

In Figure 1, a second-order fit (solid line) to the C2 and C3 height–time data (giving all data points equal weight)[2] indicates a CME lift-off time of ~0330 ± 15 UT, well before the 0406–0412 UT indicated by Reiner and Kaiser (1999) and

[2]For this and subsequent fits shown in this study, we found that ignoring the error bars on height measurements resulted in a better fit to the data. Giving equal weight to the higher data points emphasizes the deceleration and, as a result, inferred CME launch times lie closer to flare times than if the weights were taken into account. (Error bars on height measurements are also ignored for curve fits in the LASCO CME Catalog (http://cdaw.gsfc.nasa.gov/CME_list/).)

Leblanc *et al.* (2000). In any case, the inferred lift-off time based on C2 and C3 data is much earlier than the flare with 1–8 Å maximum at 0438 UT (and the metric type II onset at 0437 UT). Did the CME really lift off at ~0330 UT or ~0406–0412 UT? There is no strong activity in the GOES data for these times (Figure 1); the soft X-ray peak at ~0340 UT is ~B6. Analysis of Hα (flares and disappearing filaments listed in *Solar Geophysical Data* (*SGD*)), *Yohkoh*, and EIT data for times from ~0315–0415 UT reveals no evidence for a CME launch. A bright EIT jet from region 8100 is observed between 0359 UT and 0416 UT (indicated by arrow in Figure 2a), but no coronal response to a CME is apparent in either Figure 2a or the subsequent differenced image at 0433 UT (Figure 2b). Leblanc *et al.* (2000)

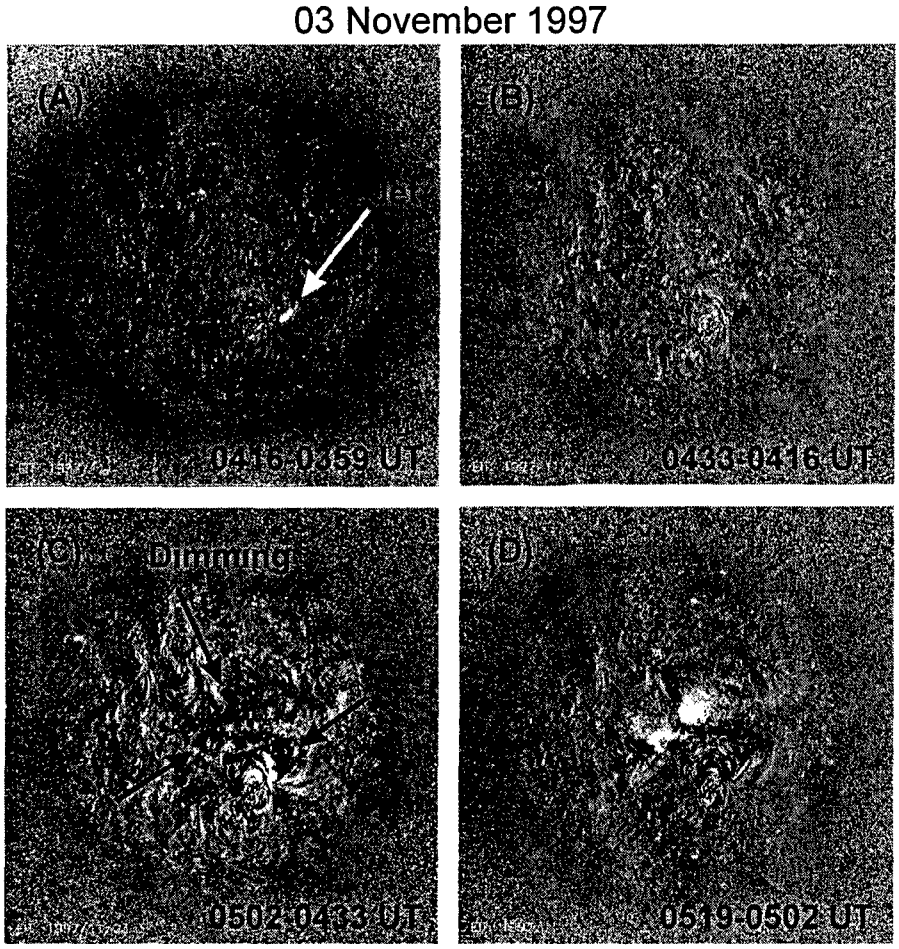

Figure 2. EIT (195 Å) running difference images for the following times: (a) 0416–0359 UT; (b) 0433–0416 UT; (c) 0502–0433 UT; and (d) 0519–0502 UT showing the coronal disturbance (in (c) and (d)) associated with the type II burst beginning at 0437 UT on 3 November 1997. The arrow in (a) indicates an EIT jet and those in (c) indicate the large scale dimming associated with the CME.

refer to an EIT wave at 0433 UT that is located 0.5 R_0 from region 8100 but such a wave is not obvious in Figure 2b, nor is it included in the list of EIT wavelike activity compiled by Biesecker *et al.* (2002) for their study.

On the other hand, there is clear evidence for a significant coronal disruption involving region 8100 that is manifested by a long-lived (>4 h) large-scale coronal dimming beginning after 0433 UT in the EIT subtraction images (arrows in Figure 2c). Such dimming regions (or transient coronal holes (Rust, 1983)) are indicators of a CME (Rust, 1983; Hudson, Acton, and Freeland, 1996; Sterling and Hudson, 1997; Zarro *et al.*, 1999; see also Hudson and Webb, 1997; Thompson *et al.*, 2000b; Harrison *et al.*, 2003). We can use observations at other wavelengths to infer with greater precision the time of explosive change in this event. Narukage *et al.* (2002) reported simultaneous waves in Hα (Moreton wave) and *Yohkoh* soft X-rays emanating from the active region with speeds of 490 ± 40 km s^{-1} and 630 ± 100 km s^{-1}, respectively. Narukage *et al.* extrapolated the positions of the wave fronts back in time to the flare site to obtain an initiation time of ~0432 UT, somewhat earlier than the onset of the sharp rise of the C8 soft X-ray flare at ~0434 UT. Narukage *et al.* (2002) suggest that this apparent timing offset (wave preceding flare) may be due to deceleration of the Moreton/X-ray waves (see Warmuth *et al.*, 2001, 2004a).

The most plausible scenario, in our opinion, for the above set of observations is that the CME was rapidly accelerated during the fast rise of the flare soft X-ray profile from 0434–0439 UT, consistent with the Zhang *et al.* (2001) analysis, and drove the Moreton and soft X-ray waves. We would expect rapid acceleration of the CME to produce a marked coronal response as manifested by the various wave phenomena and the dimming that is apparent after 0433 UT in Figure 2c. The temporal proximity of the inferred rapid acceleration phase of the CME to the type II onset at 0437 UT makes the CME a viable candidate for the metric shock driver.

In this and subsequent events, we define the impulsive rise phase of the 1–8 Å GOES profile as the interval between the start of the first minute for which the average intensity increases by at least a factor of two (above that of the previous minute) and the peak of the event. The technique is illustrated in Figure 3. Our method for identifying the onset of the flare impulsive phase applies to large, impulsive flares, such as the six considered here. It will not work for small flares which do not increase by a factor of two above background or for slow rising flares where the minute-to-minute increase in soft X-ray flux does not exceed a factor of two. In general, metric type IIs are an impulsive flare (or an impulsive phase) phenomenon (Canes and Reames, 1988; cf., Pearson *et al.*, 1989).

2.2. 03 NOVEMBER 1997, 0909 UT

This event has been analyzed in detail by Warmuth *et al.* (2001) and Khan and Aurass (2002) who present evidence indicating that the various types of wave motions observed (Moreton, EIT, soft X-ray, and metric type II burst) are closely related. In

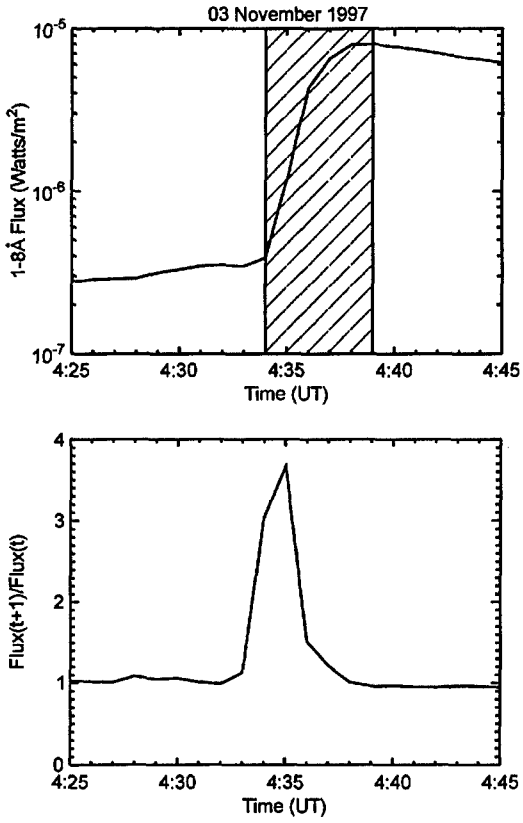

Figure 3. Top: GOES 1–8 Å light curve for the C8 flare at ~0430 UT on 3 November 1997. The soft X-ray averages are plotted at the end of the 60-second period for which the average is obtained. The hatched area indicates the flare impulsive phase corresponding to the time of rapid CME acceleration. *Bottom*: The first one-minute flux derivative value of 2 or more is used to identify the onset of the rapid rise in the soft X-ray trace.

particular, Khan and Aurass (2002) showed that the type II radio burst imaged by the Nançay radioheliograph was located in the vicinity of the Moreton, EIT, and soft X-ray waves and that the radio source exhibited motions generally consistent with those observed in soft X-rays. No CME was observed for this event, prompting Warmuth *et al.* to interpret the wave phenomena in terms of a flare blast wave. They did not take into account, however, the near central meridian location (S18W16) of the M1/1B flare, making CME observation more difficult (Webb and Howard, 1994) than is the case for near-limb events. While similar, closely preceding and following, flares from the same active region (discussed in Sections 2.1 and 2.3, respectively) had associated CMEs, making the lack of a CME problematic in this event, we note that Biesecker *et al.* (2002) have recently found a strong (~100%) association between reasonably well-defined EIT waves, such as that indicated in Figure 4b, and CMEs, suggesting that the lack of a CME in this event is indeed an

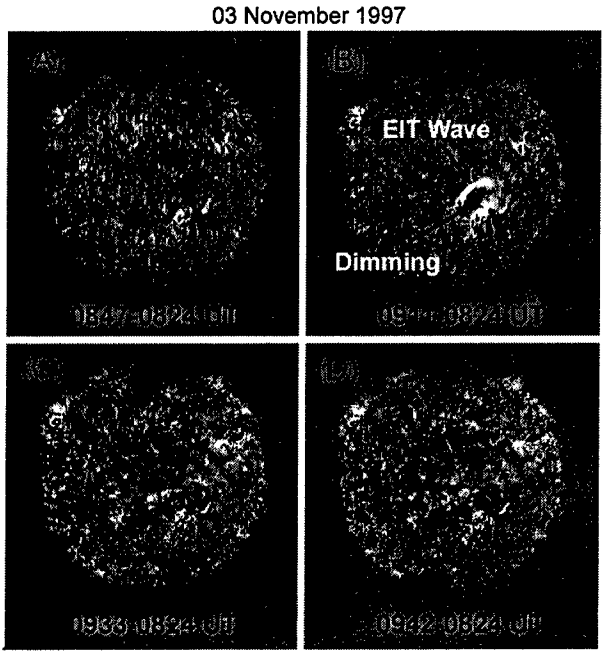

Figure 4. EIT (195 Å) base difference images for the following times: (a) 0847–0824 UT; (b) 0911–0824 UT; (c) 0933–0824 UT; and (d) 0942–0824 UT showing the EIT wave and dimming (indicated by the arrows in (b)) associated with the metric type II burst beginning at 0909 UT on 3 November 1997.

observational effect. At our request, S. Yashiro (personal communication, 2004) has re-examined this event and suggests that an enhancement above the west limb at 0953 UT, previously thought to be an internal remnant of the CME discussed in Section 2.1, may be a new CME with speed of 658 km s^{-1} (based on two data points) and lift-off time at the active region of ~0905 UT.

The Moreton, EIT, and *Yohkoh* soft X-ray waves in this event appeared to result from a disturbance at 0906 UT (Khan and Aurass, 2002) or 0907.5 UT (Warmuth *et al.*, 2001, 2004a) depending on whether a linear or a second order polynomial curve fit was used to extrapolate the distance-time points back to the edge of the flare. Both of these times fall near the onset of the 0907–0911 UT impulsive rise phase of the GOES 1–8 Å profile. Thus, following Zhang *et al.* (2001), the flare timing data, bolstered by the chromospheric and low coronal dynamics (various waves plus the dimming region between the flare site and the EIT wave (Figure 4b)), are consistent with a CME driver for the metric type II shock beginning at 0909 UT.

2.3. 03 NOVEMBER 1997, 1028 UT

This event, analyzed by Leblanc *et al.* (2000, 2001) and Reiner *et al.* (2001), is very similar to the event at 0437 UT discussed in Section 2.1. The CME height–time

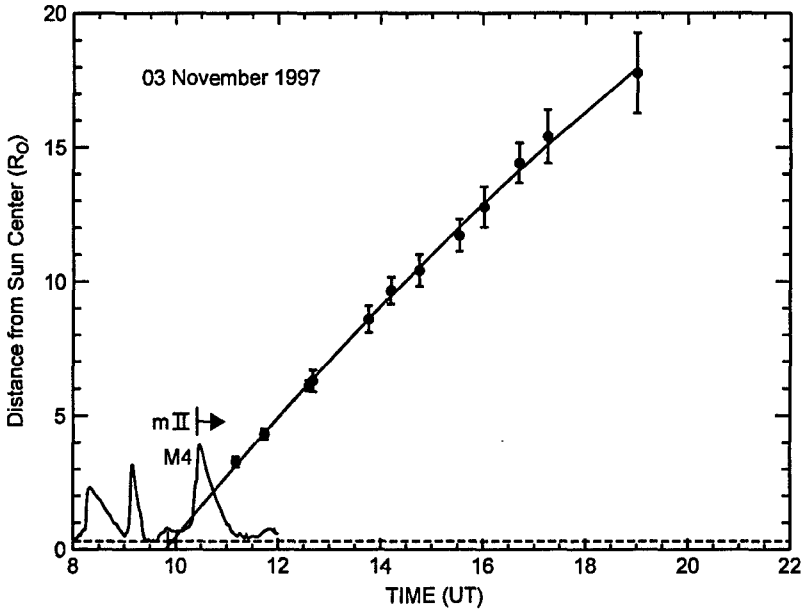

Figure 5. Height–time data for the leading edge of the CME on 3 November 1997 associated with the 1N flare (S17W22) at ~1030 UT from NOAA/USAF region 8100. The *solid line* fitted represents a constant deceleration fit to the LASCO C2 and C3 data. The *dashed horizontal line* is drawn at the projected distance of the flare from disk center. Heavy bars on this line reflect uncertainties in the lift-off time of the CME. The GOES 1–8 Å data are plotted and the onset time of the metric type II (placed at an arbitrary height) is indicated.

data and GOES soft X-ray curve are shown in Figure 5. The associated M4/1N flare was located at S17W22. A constant deceleration fit to the C2 and C3 data points extrapolated to the flare site indicates a lift-off time range from 0951–1001 UT. For comparison, Leblanc *et al.* (2000) obtain 0940–0944 UT for the lift-off time at the active region while the DH trajectory from Reiner *et al.* (2001) extrapolates back to 0939–0945 UT. All of these times are well before the onset of metric type II emission at 1028 UT. Thus both Leblanc *et al.* and Reiner *et al.* attribute the metric type II burst to a blast wave from the M4 soft X-ray flare (maximum at 1029 UT).

Is there evidence for a CME launch between ~0940–1000 UT? In SGD, Hurbanovo reports a 3N flare, with maximum at 0926 UT from region 8100, ending at 0942 UT, but this report is not corroborated by other Hα stations (Kanzelhöhe reports a SF with maximum at 0929 UT and end at 0933 UT) nor is there soft X-ray evidence for significant activity at this time with only a B5 peak at ~0950 UT. As can be seen in Figure 6, there are no significant changes between 0942 UT and 1021 UT in the EIT data.

In contrast, the rapid rise in soft X-rays at 1026 UT (following an earlier comparable (near factor of two) rise at 1022 UT during a precursor to the main event) is accompanied by an EIT wave (indicated by an arrow in Figure 6e) and long-lasting

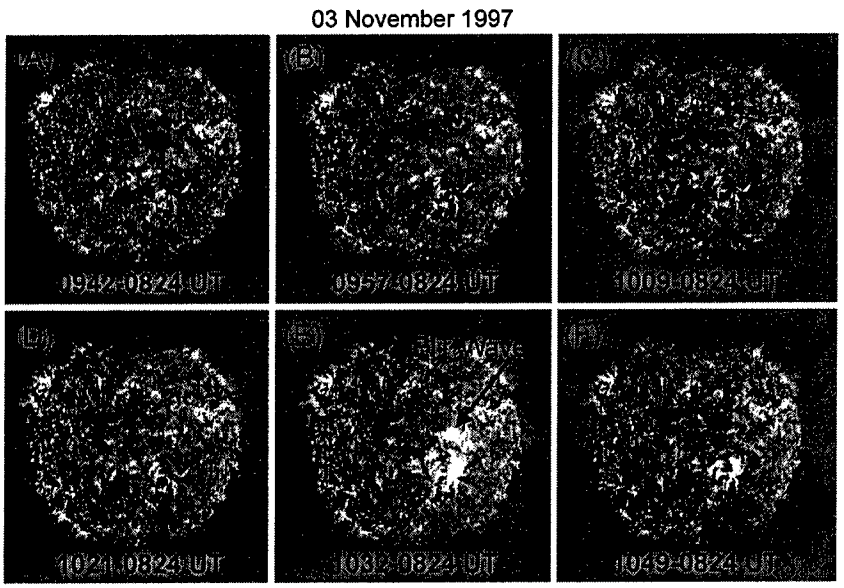

Figure 6. EIT (195 Å) base difference images for the following times: (a) 0942–0824 UT; (b) 0957–0824 UT; (c) 1009–0824 UT; (d) 1021–0824 UT; (e) 1032–0824 UT; and (f) 1049–0824 UT showing the EIT wave (indicated by an arrow in (e)) associated with the metric type II burst beginning at 1028 UT on 3 November 1997.

(>6 h) dimming beginning between 1021 UT and 1032 (Delannée and Aulanier, 1999; Klassen *et al.*, 2000; Delannée, 2000). These times bracket both the inferred rapid acceleration of the CME (1026–1030 UT) and the onset of the metric type II at 1028 UT.

2.4. 04 NOVEMBER 1997, 0558 UT

This event was discussed by Dulk, Leblanc, and Bougeret (1999) who reported that the lift-off time of the CME occurred within a few minutes of the peak time of the impulsive X2/3B flare (S14W34) and the initiation of the type II burst, both occurring at 0558 UT. Thus they were only able to conclude that the flare, the initiation of the CME, and the type II shock were intimately related and attributed the ensemble to an instability in the coronal magnetic field. Subsequently, however, Leblanc *et al.* (2001), from a consideration of the relative speeds of the CME and the type II burst, opted for a blast wave scenario. The CME leading edge height-time data for this event are shown along with the GOES soft X-ray curve in Figure 7. Dulk *et al.* obtained a lift-off time of 0552 UT (±5 min) by extrapolating a constant deceleration fit (not shown) to the limb. However, extrapolating a constant deceleration fit through the points in the figure back to the flare site yields a start time of 0534–0542 UT, well before the onset of the Hα flare at 0554 UT (and somewhat before the 0545 UT CME lift-off time obtained by Leblanc *et al.*, 2001).

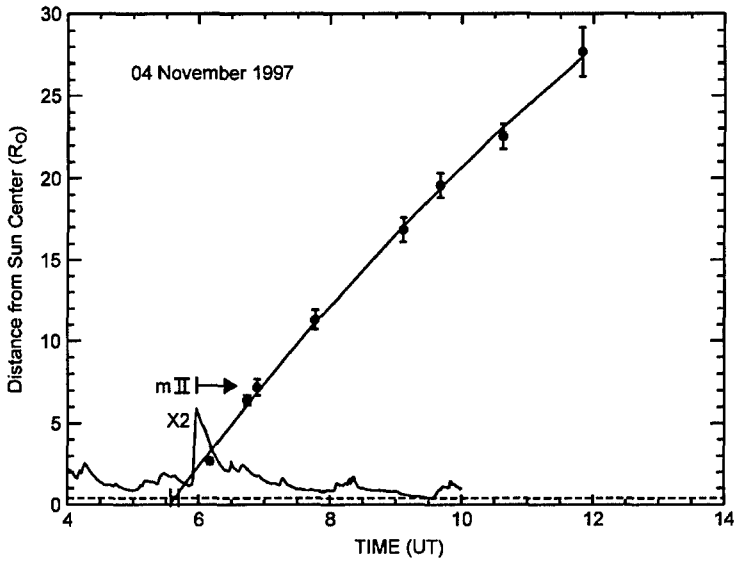

Figure 7. Height–time data for the leading edge of the CME on 4 November 1997 associated with the 3B flare (S14W34) at ~0600 UT from NOAA/USAF region 8100. The *solid line* fitted represents a constant deceleration fit to the LASCO C2 and C3 data. The *dashed horizontal line* is drawn at the projected distance of the flare from disk center. Heavy bars on this line reflect uncertainties in the lift-off time of the CME. The GOES 1–8 Å data are plotted and the onset time of the metric type II (placed at an arbitrary height) is indicated.

Is there supporting evidence for CME launch at ~0540 UT? In SGD, Urumqi reports a 2N flare from region 8100 with maximum at 0536 UT and ending at 0551 UT (C4 peak in soft X-rays at 0528 UT) but the EIT difference image in Figure 8a does not reveal any significant disruption between 0531 and 0540 UT that we might have expected to accompany the launch of a 360° halo CME. The subsequent difference image in Figure 8b (0557–0540 UT), following the X2 flare with impulsive rise phase from 0556–0559 UT, shows a major coronal disturbance. The extended bright region indicated by the arrow in Figure 8b has been characterized as a "global enhancement" by Gopalswamy *et al.* (2000a) (see Gopalswamy *et al.*, 1999a) while Delannée, Delaboudinière, and Lamy (2000) and Eto *et al.* (2002) interpret this feature in terms of instrumental scattered light. In either case, the widespread emission in Figure 8b precludes the observation of a wave (of low (Q1) confidence) and dimming in the EIT data until 0614 UT (Figure 8c). Because of the long gap (17 min) between the images in Figures 8a and 8b, a CME launch at 0545 UT (Leblanc *et al.*, 2001) cannot be ruled out on the basis of EIT data alone.

Images at other wavelengths provide support for a CME rapid acceleration phase from 0556–0559 UT as inferred from the GOES 1–8 Å light curve. *Yohkoh* partial frame images of the flare show soft X-ray motion (with speed <100 km s^{-1}) between 05:56:28 and 05:57:32 UT. Eto *et al.* (2002) observed an Hα wave for this

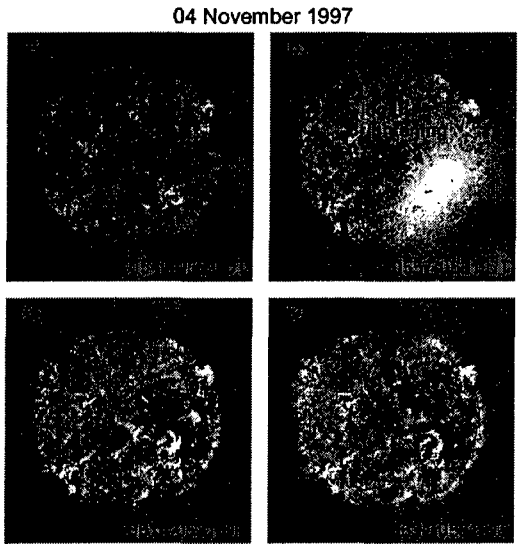

Figure 8. EIT (195 Å) base difference images for the following times: (a) 0540–0531 UT; (b) 0557–0531 UT; (c) 0614–0531 UT; and (d) 0631–0531 UT showing the "global brightening" (indicated by an arrow in (b)) and extended dimming regions (in (c) and (d)) associated with the metric type II burst beginning at 0558 UT on 4 November 1997.

event (first seen at 0558 UT at $\sim 1.2 \times 10^5$ km from the flare site) and extrapolated its trajectory back in time to an initiating disturbance at 0555 UT. (Eto *et al.* (2002) (cf., Warmuth *et al.*, 2004a) argue that the Hα wave was physically distinct from the EIT wave because of differences in timing, speed, and location between the two waves.) The soft X-ray and Hα dynamics near the fast rise in 1–8 Å intensity are consistent with the cataclysmic rearrangement of magnetic fields we would expect to be associated with the rapid acceleration of a CME. The inferred proximity of the impulsive acceleration of the $\sim$800 km s^{-1} (from a linear fit) CME beginning at 0556 UT and metric type II onset at 0559 UT make the CME a viable candidate for the type II driver.

2.5. 06 NOVEMBER 1997, 1153 UT

The CME associated with the metric type II beginning at 1153 UT (Cliver *et al.*, 2001; Leblanc *et al.*, 2001) was one of the four mass ejections analyzed in detail by Zhang *et al.* (2001). The C1 height–time data for this event are given in Figure 9. The two C1 data points indicate an average plane of sky speed of $\sim$2300 km s^{-1} for the CME between 1154.6 and 1156.7 UT. By assuming that the CME was at the solar limb at 1152 UT, the inferred onset time of the rapid acceleration phase based on soft X-ray data, Zhang *et al.* (2001) obtained an average acceleration of 7300 m s^{-2} for this event. [The 1152 UT inferred onset time lies near the reported

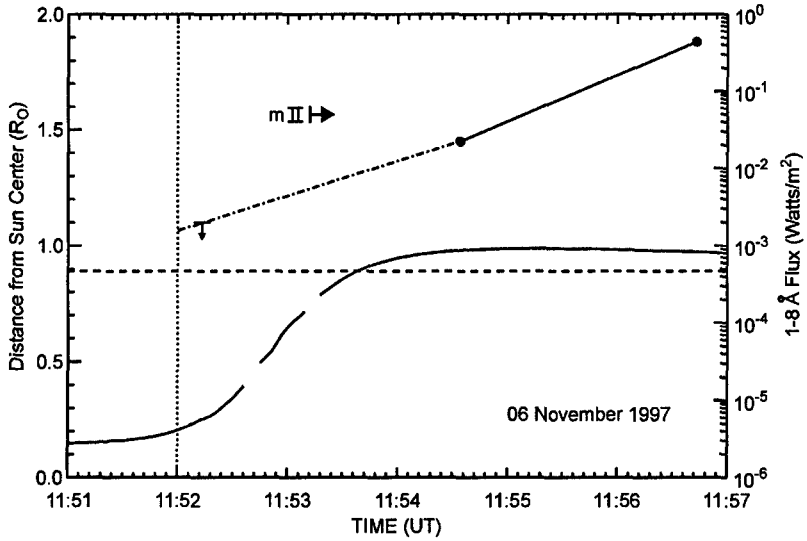

Figure 9. Height–time plot showing C1 data for the CME on 6 November 1997, with the onset time of the metric type II (placed at an arbitrary height) indicated. The *dashed horizontal line* is drawn at the projected distance of the flare from disk center. The *vertical dotted line* indicates the inferred onset time (1152 UT) of the rapid acceleration phase of the CME. The height–time plot (solid line) based on the two C1 data points is extended (*dot-dash line*) to 1152 UT through the upper limit height at 1152.2 UT to obtain the minimum average velocity and acceleration between 1152 and 1154.6 UT. High time resolution (3-second averages) GOES 1–8 Å data are plotted at the bottom of the figure.

start of decimetric/metric emission at 1151.9 UT (Maia *et al.*, 1999) and the commencement of prompt 4–8 MeV gamma-ray-line emission at 1152.6 UT (Cliver *et al.*, 2001).] The constraint provided by the upper limit height of 1.1 R_0 (corresponding to the C1 occulting disk) observed at 1152.2 UT indicates a minimum average (plane of sky) velocity of $\sim$1800 km s^{-1} between 1152 and 1154.6 UT (dot-dash extension of the C1 height–time plot), with an average acceleration of 11,500 m s^{-2}. For comparison, Gallagher, Lawrence, and Dennis (2003) obtained a peak acceleration of $\sim$1500 m s^{-2} for the fast ($\sim$2500 km s^{-1}) CME on 21 April 2002.

Yohkoh SXT images provide supporting evidence for rapid CME acceleration between 1152–1156 UT. Nitta, Cliver, and Tylka (2003) analyzed the SXT data for this event and reported fast (>2000 km s^{-1}) but very faint motions during the flare impulsive phase (between 11:53:28 and 11:54:16 UT). In contrast, at the extrapolated CME lift-off time range of 1145–1150 UT (at the S18W63 flare site) obtained by Leblanc *et al.* (2001) from a constant deceleration fit to C1–C3 data, no significant soft X-ray changes were observed by *Yohkoh* SXT. Using a density model and radio spectrograph data, Leblanc *et al.* (2001) found that the type II burst lagged behind the CME leading edge in the low corona and argued that the shock only became CME-driven beyond $\sim$30 R_0. Given the uncertainty in density models, however, the fact that the $\sim$2000 km s^{-1} CME was in the nominal height

range of metric emission during the time of the low coronal type II burst makes it difficult to rule out the CME as the metric shock driver.

2.6. 27 NOVEMBER 1997, 13:16 UT

This event analyzed by Klein *et al.* (1999) is important because it is the premier example of a metric type II burst with a candidate flare ejecta driver. Klein *et al.* showed that the non-radial motion of a soft X-ray loop observed by the *Yohkoh* SXT was overlain with a type II source imaged at Nançay. A straight line extrapolation of C2/C3 coronagraph data (filled circles and solid line in Figure 10) indicates that the projected height of the CME leading edge was at $>1\,R_0$ at the onset of the metric type II (1316 UT), well above the imaged type II source region height of $\sim 10^5$ km, apparently ruling out a CME driver (as was concluded in Cliver and Hudson, 2002). However, this event was also analyzed by Leblanc *et al.* (2001) who included the C1 coronagraph data in their analysis and deduced that the metric type II shock could have been CME-driven. Difference images of the CME in C1 are given in Figure 11 where the leading edge of the CME is indicated in (b) and (c). When

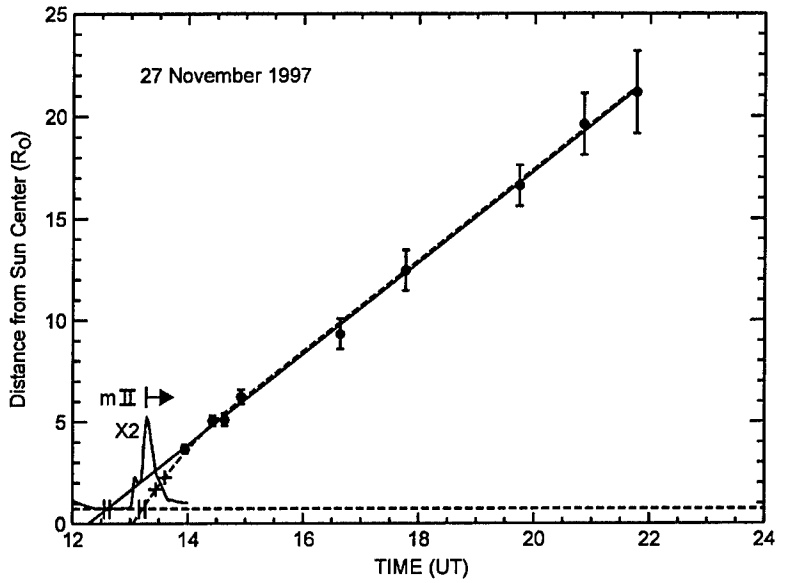

Figure 10. Height–time data from C2 and C3 for the leading edge of the CME on 27 November 1997 associated with the 2B flare (N16E63) at ~1300 UT from NOAA/USAF region 8113 (filled circles). The solid line fitted represents a constant deceleration fit to the LASCO C2 and C3 data. The *dashed line* fit (see text) takes into account C1 data points (+ signs). The *dashed horizontal line* is drawn at the projected distance of the flare from disk center. Heavy bars on this line reflect uncertainties in the lift-off times of the CME for the two fits. The GOES 1–8 Å data are plotted and the onset time of the metric type II (placed at an arbitrary height) is indicated.

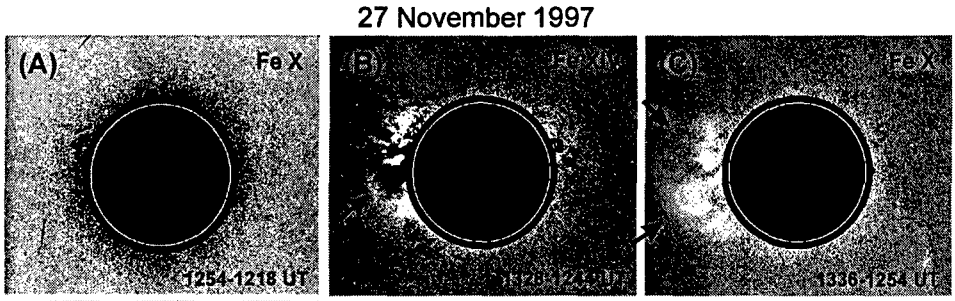

Figure 11. Difference images from the LASCO C1 coronagraph for the CME associated with the metric type II burst at 1316 UT on 27 November 1997: (a) 1254–1218 UT (6374 Å); (b) 1328–1244 UT (5302 Å); and (c) 1336–1254 UT (6374 Å). The position of the leading edge is indicated by arrows in (b) and (c).

these two points (+ signs) are added to the height–time plot, a constant deceleration (-73 m s^{-2}) fit to the first six data points combined with a constant velocity ($\sim$435 km s^{-1}) fit to the five later points (composite fit shown by dashed line in Figure 10) yields an inferred lift-off time at the flare site (N16 E63 in NOAA/USAF region 8113) of 1309–1316 UT. These times partially overlap the rapid rise phase (1313–1318 UT) of the soft X-ray curve for the X2/2B flare (the Hα start time is 1301 UT and there is a soft X-ray precursor (C3 peak at 1306 UT) to the main event).

In simplified constant deceleration (or linear) fits such as used in Figure 10, the positive CME acceleration low in the corona is contained in the initial velocity (V_0). In this case $V_0 = 850$ km s^{-1}. A realistic fit, requiring more data points, should yield an "S-shaped" height–time profile (e.g., Gallagher, Lawrence, and Dennis, 2003).

The series of EIT running-difference images in Figure 12 reveals a similar pattern to that seen for previous events in this study – an absence of coronal activity near the time of CME launch inferred from a straight line extrapolation to the solar surface (1233–1239 UT; solid line in Figure 10) and evidence for coronal dynamics near the time of rapid acceleration of the CME (1313–1318 UT). Klein *et al.* (1999) report the onset of soft X-ray loop expansion at $\sim$1316 UT (and motion of a localized brightening ("blob") within an active region loop with speed $\sim$800 km s^{-1} as early as 1312.3 UT). EIT dimming (arrow in Figure 12d) and a low confidence (Q1) EIT wave are first apparent in the 1337–1311 UT difference image (Figure 12d) as indicated on the EIT wave list compiled for the Biesecker *et al.* (2002) study, although Klassen *et al.* (2000) report that the wave was first observed at 1311 UT (Figure 12c).

The metric type II burst in this event has a high starting fundamental frequency of $\sim$250 MHz. Vršnak and Lulić (2000a) have argued that even flare sprays develop too slowly to drive such high-frequency type II bursts and that therefore such events must result from blast wave shocks. However, the combined *Yohkoh* soft X-ray and Nançay radio evidence for a material (non-blast wave) driver in this event undercuts

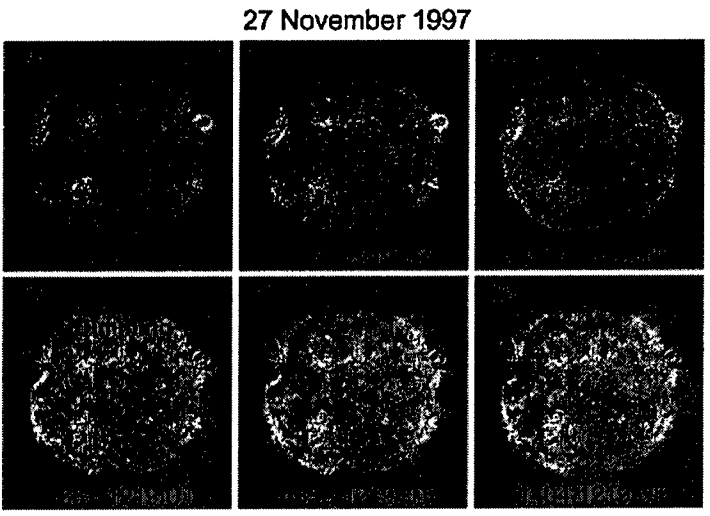

Figure 12. EIT (195 Å) base difference images for the following times: (a) 1235–1219 UT; (b) 1250–1219 UT; (c) 1311–1219 UT; (d) 1337–1219 UT; (e) 1352–1319 UT; and (f) 1404–1319 UT showing the EIT dimming (indicated by an arrow in (d)) associated with the metric type II burst beginning at 1316 UT on 27 November 1997.

this argument. If the shock is driven by the CME, it implies that the CME originates in a relatively small structure, with scale size $\sim 10^5$ km.

2.7. Coronal Dynamics Associated with Metric Type II Burst Origins

In this section we summarize the various types of low coronal dynamics observed in association with the inferred CME rapid acceleration phase for the six events under consideration. Occurrence and timings of the flares, metric type II bursts, CMEs, ejecta, waves, and dimmings are given in Table I where it can be seen that mass and wave motion were general characteristics of the events. The timing relationships between the phenomena are illustrated in superposed epoch form in Figure 13 where the zero epoch is taken to be the onset time of the inferred rapid acceleration phase of the CME based on the GOES 1–8 Å flare soft X-ray curves. It has long been recognized (e.g., Neupert, 1968; Kane, 1974; Dulk, McLean, and Nelson, 1985) that the onset of the main phase of the flare soft X-ray emission is closely aligned with the flare impulsive phase, which is characterized by hard X-ray, microwave, and metric type III bursts. Gallagher, Lawrence, and Dennis (2003) recently showed that onset of the rapid acceleration phase for the 21 April 2002 CME coincided with the start of >25-keV X-ray emission and peak acceleration occurred near the hard X-ray flux maximum, well before the soft X-ray peak. In Figure 13, the CME rapid acceleration phase (prompt rise phase of the soft X-ray burst) is shaded and we have indicated the time of first observation of the

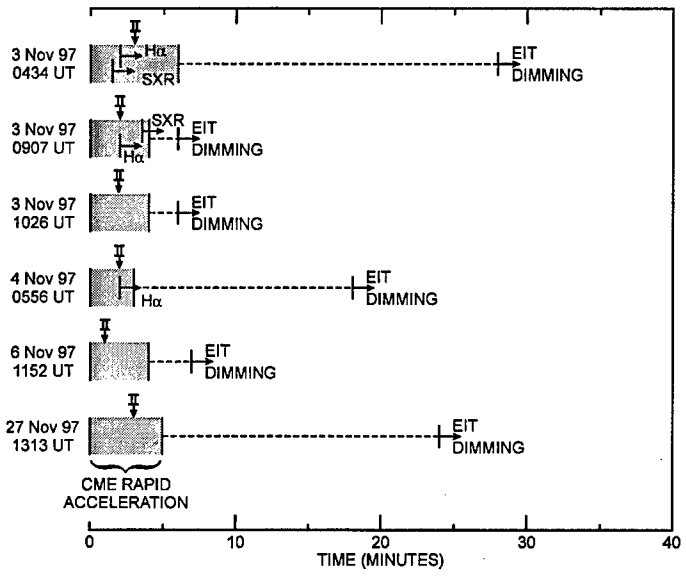

Figure 13. Superposed epoch plot for the six events considered in this study with the onset of the flare impulsive phase (start time of the inferred rapid acceleration of the CME) as the zero epoch. Onset times of Moreton (Hα), EIT, and soft X-ray (SXR) waves are indicated as well as the onset times of EIT dimmings.

various waves (soft X-ray (SXR), EIT, Hα), the dimmings, and the type II bursts. (We have not shown the times of soft X-ray ejecta in Figure 13 because in each case the ejecta (or possible ejecta) fall within/near the shaded region of the time lines.) The EIT observations are hampered by relatively poor time resolution but for three of the cases, EIT waves and dimmings are observed within 5 min of the end of the rapid acceleration phase of the CME. In no case are waves or dimmings observed before the start of this phase. The close correspondence between the onset of the Moreton wave in the three cases for which Hα waves were reported and the onset of metric type II emission (within 1 min in all cases; Table I) has been pointed out by Warmuth *et al.* (2004b) for a larger sample containing these three events (see also Smith and Harvey, 1971).

In sum, the data are consistent with CME drivers for all of the various waves as well as the metric type II shocks. Again, we would expect the abrupt acceleration of a CME to produce a significant coronal response, such as the waves and dimmings observed.

There is an additional reason to believe that the wave phenomena in these six events are CME-driven. In Table I, the classification scheme for dimmings (West and Thompson, 2003) is based on the temporal/spatial relationship between the EIT waves and the dimmings. Dimming classifications of D4 and above imply a reasonable or better correspondence between the dimming and the wave, such that one could guess the morphology of one from knowledge of the other. Five of the

six events (all except 3 November 1997 at 1028 UT)[3] had dimming classifications of D4 or greater. In general, for these cases, the wave precedes the dimming region as it propagates across the disk. As pointed out by Thompson *et al.* (2000a) in their analysis of the 24 September 1997 EIT waves and dimmings, this behavior suggests that the waves are driven, at least initially, by CMEs. Quoting from Thompson *et al.*, "The gradual formation of the dark depleted region could represent an expanding driver of the bright front, with the dimming region (CME) causing the bright front to form." This behavior is clearly seen in Figure 4 for the event on 3 November discussed in Section 2.2 above.

Thompson *et al.* (2000a) speculated that EIT waves might become freely propagating in their later stages. The two EIT waves on 24 September 1997 that they analyzed began as bright, sharp compact fronts "wrapped around" a dimming region and were subsequently observed as weak diffuse propagation fronts that left little evidence of their transit from one EIT image to the next. Similar evolution is observed for the event in Figure 4. This behavior is consistent with an early driven stage of wave development followed by a freely-propagating phase. Warmuth *et al.* (2001, 2004a,b) report that flare-associated wave phenomena exhibit deceleration, perturbation profile broadening, and amplitude decrease with time. In addition EIT waves are observed to avoid high Alfvén speed regions (Thompson *et al.*, 1999; Wills-Davey and Thompson, 1999; Ofman and Thompson, 2002; see also Uchida, Altschuler, and Newkirk, 1973). Each of these characteristics is symptomatic of freely-propagating waves (although, as Warmuth *et al.* (2004b) note, the evolution of a piston-driven wave depends strongly on the piston kinematics).

An alternative view of the close temporal/spatial relationship between dimmings and waves reported by West and Thompson (2003) is that the dimmings are rarefaction regions behind the waves (Landau and Lifshitz, 1987). We discount this interpretation because any such dimming would be short-lived, with a duration on Alfvén time scales, whereas the dimmings lying close to the flare sites in the November 1997 events persisted for ~4–12 h after the eruption.

2.8. Initial Size of CMEs

One implication of our result is that certain CMEs start life as relatively small structures with inferred initial sizes $\sim 10^5$ km. C1 measurements at 11:52:13 UT (Zhang *et al.*, 2001) for the 6 November 1997 event in Figure 9 show that near the onset of the rapid acceleration phase (1152 UT), the radial height of the CME was less than 1.3×10^5 km. Extrapolating back from the first measurement of the CME leading edge ($1.45\,R_0$) at 11:54:34 UT using a radial velocity of 2,600 km s^{-1} indicates a radial height of 4×10^4 km at 1152 UT. Within the C1 coronagraph field

[3]Delannée and Aulanier (1999) and Delannée (2000) base their alternative interpretation of EIT waves as essentially stationary objects in part on this event.

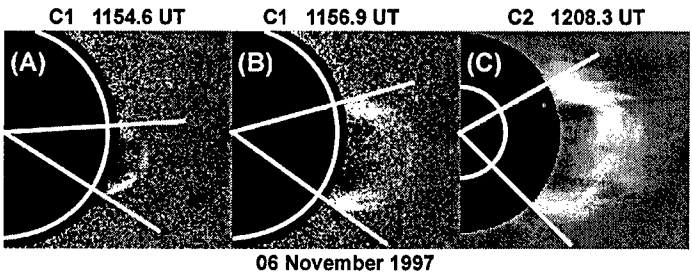

Figure 14. SOHO LASCO images of the CME on 6 November 1997: (a) C1: 1154.6 UT (b) C1: 1156.9 UT; and (c) C2: 1208.3 UT. The white semicircle on the occulting disk marks the limb of the Sun and the white lines from Sun center indicate the lateral expansion of the CME in time.

of view, the angular width of the 6 November 1997 CME expands from ~ 35° (at 11:54:34 UT) to ~50° (11:56:43 UT) in 2.3 min and is ~75° wide at its first image in C2 (12:08:20 UT) (as indicated by white lines in Figure 14a–14c). The inferred size of the CME is less than 20° at ~1152 UT (based on a linear extrapolation of the two C1 data points in a width versus time plot). Maia *et al.* (1999) reported a corresponding lateral expansion in the radio sources observed for this event.

The expanding soft X-ray loop observed in the 27 November 1997 event analyzed by Klein *et al.* (1999) had a scale height of 10^5 km. A structure with length of $\sim 2 \times 10^5$ km will subtend an arc of ~15° on the solar surface, well below the ~45° median angular span of CMEs measured by the coronagraph on the Solar Maximum Mission (SMM; Hundhausen, 1993; St. Cyr *et al.*, 1999) and the widths (91°, 109°, 122°) listed in the LASCO CME catalog for the three non-halo events in Table I. The large final angular spans of the Table I CMEs presumably result either from lateral expansion or by destabilization of adjacent/over-lying large-scale structures such as trans-equatorial loops (Delannée and Aulanier, 1999; Khan and Hudson, 2000). Zhang *et al.* (2004) suggested that the disparity between flare region size and CME size is caused by the super-expansion of the CME in the low corona during its acceleration phase, and that expansion can be non-radial.

Evidence for smaller initial sizes for CMEs have been presented by Dere *et al.* (1997) who found that a CME on 23 December 1996 that eventually spanned 70° in latitude originated in a volume with dimensions of $\sim 2.5 \times 10^4$ km, and Gallagher, Lawrence, and Dennis (2003) who used Transition Region and Coronal Explorer (TRACE) images at 195 Å to obtain an initial height of $\sim 2 \times 10^4$ km for a CME with a final reported angular span of ~240°.

The small initial CME sizes we infer for the events in our study reflects the impulsive nature of the associated flares. In general, we would expect CMEs associated with flares with longer time scales to originate in larger volumes.

The starting fundamental frequencies of the six metric type II bursts in Table I ranged from 115 MHz to 250 MHz. For a 5× Saito density model (Robinson, 1985), these frequencies indicate a range of starting radial heights from

0.7–2.2 $\times$ 10^5 km, with uncertainties (based on 2$\times$ and 10$\times$ Saito models) of approximately $\pm$0.5–1.0 $\times$ 10^5 km for the individual cases. (These radial heights are of the same order as the lateral displacements of the Moreton waves from the flaring region ($\sim 10^5$ km) for the three cases where such waves were observed (Table I).) Where was the CME leading edge at the onset of the metric type II emission? As the case studies in Sections 2.1–2.6 make clear, CME positions below the C2 occulting disk cannot be accurately determined without low coronal observations. For the 6 November CME, the most constrained event in our sample (highest C1 cadence near CME launch), the inferred CME radial height at the onset of the type II burst at 1153.2 UT is 2.3 $\times$ 10^5 km, in comparison with a type II starting height of 7 $\pm$ 6 $\times$ 10^4 km inferred from the burst starting frequency (250 MHz). While this comparison is apparently inconsistent with the CME-driver hypothesis, the various uncertainties/unknowns involved (e.g., coronal density structure, actual CME trajectory, location of type II emitting region relative to CME leading edge (see Sections 3.2 and 3.3 below) are significant.

3. CMEs and Type II Shocks: Other Aspects

In the following subsections we briefly review various lines of evidence that bear on the relationship between CMEs and metric type II bursts.

3.1. CME–METRIC TYPE II ASSOCIATIONS

For the 1979–1985 period of Solwind coronagraph observations, Cliver *et al.* (1999) reported a 64% (49/76) degree of association between metric type II bursts associated with limb flares ($\geq 60^\circ$ from central meridian) and coronal mass ejections. The associated CMEs all had speeds $\geq$400 km s^{-1}. More recently, N. Gopalswamy, D. Hammer, and colleagues (N. Gopalswamy, personal communication) using data from the LASCO C2 and C3 coronagraphs on SOHO, obtained a 93% (90/97) degree of association between near-limb type IIs and CMEs. (Classen and Aurass (2002) reported a lower percentage association between metric type IIs and CMEs but they did not consider the location of the associated flare). The average/median speeds of the CMEs were 813 km s^{-1}/$\sim$650 km s^{-1}. In contrast to Cliver *et al.*, Gopalswamy and colleagues found that 20% of the associated CMEs had speeds $<$400 km s^{-1} ($>$200 km s^{-1} in all cases).

Other, less direct, association studies provide additional evidence for a close link between CMEs and metric type II bursts, particularly the combination of: (1) the investigation by Klassen *et al.* (2000) showing that at least 90% (19/21) of type II bursts observed with the Potsdam spectrograph during 1997 were accompanied by EIT waves (see Gopalswamy *et al.* (2000b) for imaging evidence for an EIT wave/metric shock link); and (2) the study by Biesecker *et al.* (2002), based on EIT observations between March 1997 and June 1998, showing that all (11/11)

favorably located (longitude >60°), high-quality ($Q \geq 3$) EIT waves were associated with CMEs. Although the number of events on which Biesecker *et al.* based their conclusion was relatively small, they regarded the correlation between EIT waves and CMEs as "very strong" and stated, "If an EIT wave is observed, there must be a CME; however the converse is not necessarily true."

In arguing against a blast wave origin for metric type II shocks, Cliver *et al.* (1999) emphasized the lack of correlation between flare size and type II occurrence, echoing arguments made by Roberts (1959) 40 years earlier that a "special condition" was needed to distinguish the flares in a given size range that had type II association from the vast majority (for all but the largest size bins) that did not. Many type IIs are associated with relatively weak flares which nonetheless have fast CMEs. Cliver *et al.* noted that the well-studied event of 12 May 1997 (Thompson *et al.*, 1998) fit this description. The C2 flare was accompanied by a ~450 km s^{-1} full halo CME originating near central meridian, a ~15 min type II burst, and an EIT wave and coronal dimming that encompassed much of the visible solar hemisphere. Another example of a metric type II burst and EIT wave associated with a small flare is the 27 January 1998 event reported by Gopalswamy and Thompson (2000). The B2 soft X-ray peak of this event (indicated by an arrow in the top of Figure 15)

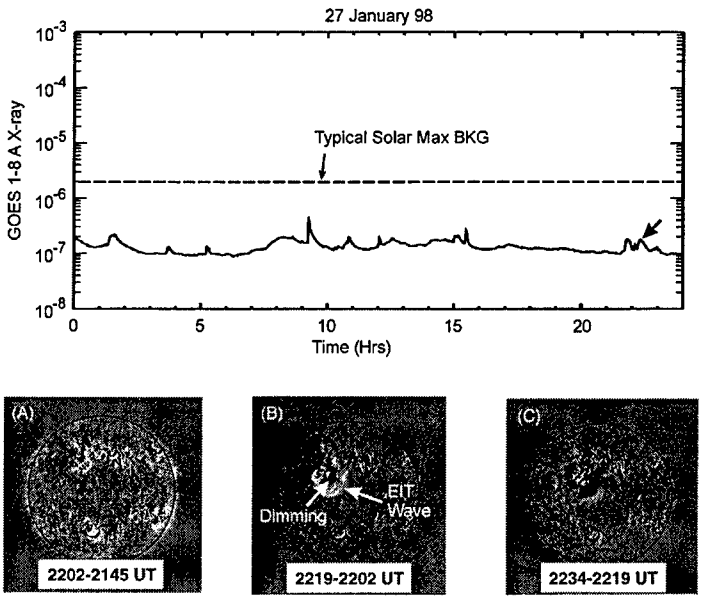

Figure 15. Top: GOES 1–8 Å soft X-ray profile for 27 January 1998. The time of the B2 eruptive flare depicted in the bottom of the figure is indicated by an arrow. The *dashed horizontal line* gives the typical 1–8 Å background at solar maximum. *Bottom*: EIT (195 Å) running difference images for the following times: (a) 2202–2145 UT; (b) 2219–2202 UT; and (c) 2234–2219 UT showing the EIT wave and dimming (indicated by arrows in (b)) associated with the type II burst beginning at ~2215 UT on 27 January 1998.

would be an order of magnitude below the 1–8 Å background level typically observed for active periods near solar maximum. As can be seen in the GOES 1–8 Å plot for this date, several soft X-ray bursts of this size or larger occurred during the day but only one was associated with a type II burst. Not coincidentally, in our opinion, the B2 burst beginning shortly after 2200 UT was the only one also associated with a well-defined EIT wave and dimming (bottom of Figure 15 (panel b)) and an inferred (via the EIT wave and dimming) CME (no associated CME was observed but the flare was located close to disk center; both the LASCO and EIT instruments had uninterrupted coverage during this day, at normal cadence). If such small flares by themselves (i.e., without an accompanying CME) could cause type II bursts, type IIs would occur far more frequently than is observed.

Before leaving this section, it is important to note that a fast CME is not a sufficient condition for a type II burst to occur. Approximately one-third of fast (>500 km s^{-1}) Solwind CMEs lacked metric shocks (Sheeley *et al.*, 1984; Kahler *et al.*, 1984). Low Alfvén speed above an active region has been suggested as an alternative (additional) special condition for metric type II shocks (Uchida, 1973, 1974; Kahler *et al.*, 1984). Recent investigations of the Alfvén speed profile above active regions and its effect on type II shock formation have been made by Mann *et al.* (1999), Gopalswamy *et al.* (2001), Gopalswamy and Kaiser (2002), and Vršnak *et al.* (2002).

3.2. Connectivity of metric and DH type IIs

The question of the relation of metric type IIs observed by ground-based instruments to DH type IIs observed by the *Wind*/WAVES experiment has been closely tied to the debate over the origin of type IIs (see the exchange between Cliver (1999) and Gopalswamy *et al.* (1999b)). To summarize, since it is generally accepted (Cane, Sheeley, and Howard, 1987; Bale *et al.*, 1999; Gopalswamy *et al.*, 2000a; cf., Vršnak and Lulić, 2001) that DH and lower frequency type II shocks are CME-driven, type II emission extending smoothly from the metric range to the 14 MHz upper frequency of the *Wind*/WAVES experiment would imply that the associated metric type II was CME-driven as well. On the other hand, "disconnects" between shocks in the two frequency ranges could be consistent with different shock origins.

Reiner and colleagues have written a series of papers (Kaiser *et al.*, 1998; Reiner and Kaiser, 1999; Reiner *et al.*, 2000, 2001) drawing attention to apparent mismatches in the trajectories (speeds and launch times) of metric and DH type II bursts. Five of the November 1997 events we considered had DH type II components and published radio records for three of these events [3 November 0437 UT and 1028 UT, Plates 1 and 2, respectively, in Leblanc *et al.*, 2000; see also Reiner and Kaiser (1999) and Reiner *et al.* (2001); 4 November 0558 UT, Figure 1 in Dulk,

Leblanc, and Bougeret, 1999] exhibit abrupt decreases in their apparent velocities, a behavior exhibited by ~15% of type II bursts (Robinson, 1985). Like the three November 1997 events, the type II bursts that displayed apparent speed decreases in Robinson's sample were characteristically associated with impulsive flares with soft X-ray durations of one hour or less. Extrapolations of the height–time plots of metric and DH type IIs for the events on 3 and 4 November indicate separate launch times for the initiating disturbances, with the inferred DH shock initiator (presumed to be a CME) launch time occurring well before the associated flare and metric type II burst. In general, such differences in apparent launch times for metric and DH type II exciters have been interpreted in terms of two different types of shocks, specifically flare blast (or ejecta-driven) waves for the metric type IIs and CME-driven shocks for the DH type IIs (e.g., Reiner and Kaiser, 1999; Leblanc *et al.*, 2000, 2001; cf., Robinson, 1985).

As shown above, however, the Zhang *et al.* (2001) result and low coronal observations indicate a close timing association between the fast rise of soft X-ray emission and the rapid acceleration phase of the CME in the six impulsive events studied here, thereby removing the CME–type II timing problem and making CMEs a viable candidate for metric shock drivers in these events. The problem then becomes one of explaining apparent changes in shock trajectories for events such as those at 0437 UT and 1028 UT on 3 November 1997 and 0558 UT on 4 November 1997 in terms of the single CME-driver picture for m/DH type II bursts. Surprisingly, certain type II bursts which exhibit such changes, e.g., the three November events or the event on 19 May 1998 (Reiner and Kaiser, 1999), can still give the appearance of being a single entity. Leblanc *et al.* (2000) suggested that the separate metric (blast wave) and DH (CME-driven) components of the events on 3 November 1997 that they analyzed may have merged at a height of $\sim 2\,R_0$ and propagated outward as a CME-driven shock thereafter. While our re-examination of the CME dynamics in these events undercuts their blast wave hypothesis for the metric type IIs, their view of the metric/DH type II as a connected event supports our general thesis. The 19 May 1998 event (Figure 16) analyzed by Reiner and Kaiser (1999) and commented on by Gopalswamy (2000) also deserves mention in this context. Reiner and Kaiser interpreted this event in terms of separate metric and DH shocks (based on differences in inferred initiator launch times), while Gopalswamy (2000), from visual inspection, arrived at the opposite conclusion that "some DH IIs are extensions of metric type IIs".

In a CME-driven-shock scenario for events like that in Figure 16 (an eruptive prominence (Subramanian and Dere, 2001) associated with a B7 soft X-ray flare but a 800 km s^{-1} CME), possible causes of the apparent decrease in speed as the shock moves outward in the solar atmosphere include: (1) shock (CME) deceleration; (2) increase in the Alfvén Mach number above a critical value, resulting in turbulence and shock dissipation (Karlický *et al.*, 1982); (3) a change in the direction of shock propagation from radial to non-radial; (4) a decrease in the density gradient in the type II source region (Robinson, 1985) based on the qualitative picture of Wagner

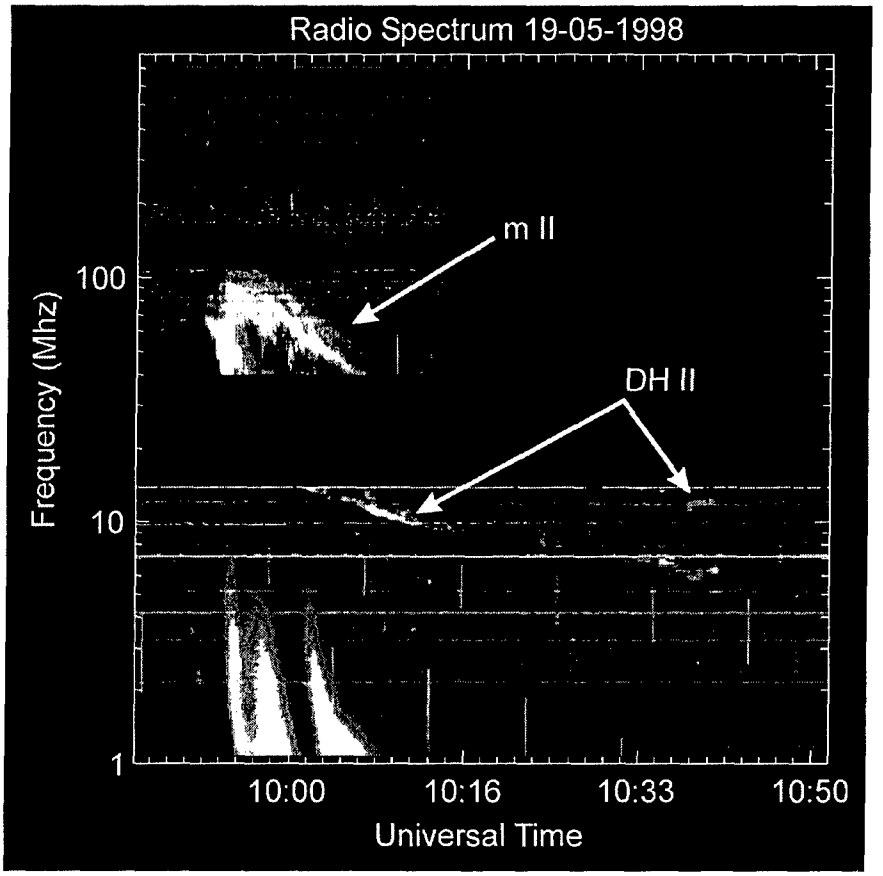

Figure 16. Composite of a type II burst observed in the metric range with the Potsdam spectrograph and in the DH range by the WAVES/RAD2 experiment on *Wind* (adapted from Gopalswamy, 2000). Fundamental and harmonic components are observed in both wavelength ranges.

and MacQueen (1983) for type II shock formation; and (5) shock-drift electron acceleration (Holman and Pesses, 1983) at the flanks of a CME resulting in initial high speed of the type II source followed by deceleration (Steinolfson, 1984, 1985). In addition, apparent disconnects between metric and DH type II bursts could result if a single CME-driven shock simultaneously traverses regions of different density (Raymond *et al.*, 2000; cf., Reiner *et al.*, 2000). In sum, apparent (or not so apparent, Figure 16) disconnects between metric and DH shock trajectories for individual cases need not be taken as evidence for separate (blast wave and CME) shock drivers in a single event. The same caveat holds for statistical evidence supporting disconnects between CMEs and metric type II shocks (e.g., Gergely, 1984) or between metric and DH type II bursts (Reiner *et al.*, 2001).

Recently, Reiner *et al.* (2003) have presented a detailed analysis of a type II burst on 20 January 2001 that was observed at both metric (starting fundamental

frequency of 160 MHz) and DH wavelengths that they interpreted in terms of a single CME-driven shock. These authors used Mauna Loa coronagraph data (occulting disk at 1.08 R_0) that enabled them to confidently link the metric type II burst to the CME. Reiner *et al.* argue that there was "no obvious relationship" between the CME lift-off time and the associated flare, but in fact their CME launch time of 2110.2 UT occurred essentially simultaneously with the first rapid (~2×) increase in the 1–8 Å flux of the associated flare at 2110 UT and a >1000 solar flux unit microwave burst with a start time of 2110 UT and a peak time of 2112 UT is reported in SGD.

3.3. Spatial relationship between CMEs and metric IIs

Next to the timing problem addressed in this study, the main challenge for the CME-driver scenario for metric type II bursts has come from radio-imaging and spectrographic studies bearing on the spatial relationship of the CME to type II emission. While there are reported (e.g., Robinson and Stewart, 1985) cases where the shock source is located at or near the CME front, several studies (e.g., Gergely *et al.*, 1984; Gary *et al.* 1984; Leblanc *et al.* 2001) indicate that type II emission occurs at the flanks of the CME or behind its leading edge.

Recently, Mancuso and Raymond (2004) have used ultraviolet coronagraph spectrometer (UVCS) observations aboard SOHO to deduce characteristic offsets of metric type II emission behind the CME leading edge, consistent with the result of Gary *et al.* Mancuso and Raymond obtained ambient coronal electron density profiles for 29 metric shock events occurring from March through December 1999. The time proximate and position angle specific density profiles they obtain are preferable to standard models (e.g., Newkirk, 1961; Saito, 1970; Leblanc, Dulk, and Bougeret, 1998) that are based on averaged observations. These profiles enabled the authors to confidently determine type II trajectories that they then compared with CME height–time plots. A comparison of the times that the CME leading edges and type II shocks crossed the 1.8 R_0 level in the solar atmosphere showed that the CME typically traversed this altitude ~10 min (range from ~−15 (type II leads) to +35 min (CME leads)) before the metric shock. (For a CME speed of 500–1000 km s^{-1}, this corresponds to a spatial offset of ~0.4–0.8 R_0.)

Mancuso and Raymond (2004) suggest that the apparent lag between CME leading edge and the type II source could be a geometrical effect. They note that shock strength will be enhanced along streamer axes (because of their lower Alfvén speeds) and that such streamers are characteristically offset from the axis of symmetry along which the CME propagates. The net result, for a shock wrapped around the CME leading edge, is that type II emission will appear to lag the CME. This geometrical model finds support from an earlier study by Stewart (1984) based on Culgoora observations in which type II emission characteristically overlay filaments and filament channels adjacent to active regions, rather than the associated flares.

As Mancuso and Raymond (2004) note, the time lag they obtained between CME and metric shock crossings of the 1.8 R_0 level is based on extrapolation of C2 and C3 CME data that ignores strong positive accelerations below the C2 field of view. For an example of how significant this effect can be, the time difference between the CME crossing of the 1.8 R_0 level for a fit based on C2/C3 data and one which incorporates C1 data for the 27 November 1997 event (Figure 10) is ~30 min.

To summarize this section, radio imaging and spectrographic evidence to date (Gary *et al.*, 1984; Leblanc *et al.*, 2001; Mancuso and Raymond, 2004) indicates that metric shocks characteristically lag behind the CME leading edge, although such factors as coronal and shock geometry (quasi-parallel or quasi-perpendicular) as well as the CME trajectory below the C2 occulting disk may yet make it possible to reconcile the observations with the CME driver scenario.

4. Summary

In Section 2, we re-examined solar circumstances for six metric type II bursts during November 1997 that have figured prominently in the debate over the origin of slow-drift solar radio bursts. In general, these events have provided evidence for non-CME drivers for type II bursts. For certain of these events, extrapolations of height–time plots based on observations of CME leading edges in LASCO C2 and C3 coronagraph data indicated CME launch times up to 25–45 min before the flare impulsive phase, well before type II onset, leading previous authors to argue against a CME driver. Thus, for example, Leblanc *et al.* (2000) concluded that the type II shocks near 0430 and 1030 UT on 1997 November 3 "were clearly not driven by CMEs; ... they were blast waves which faded out at $< 4\ R_0$" (see also Reiner and Kaiser, 1999; Reiner *et al.*, 2001). For the 1997 November 27 event, Klein *et al.* (1999) used radio and soft X-ray images to tentatively identify the type II driver with a soft X-ray "blob". Another of these events (1997 November 3, 0909 UT) was used as evidence for a blast wave origin for EIT and Moreton waves (Warmuth *et al.*, 2001).

Our re-examination of these events was prompted by the recent study of Zhang *et al.* (2001) who used LASCO C1 coronagraph data to show that the rapid acceleration phase of CMEs corresponded to the fast rise of the flare soft X-ray light curve. Using this new tool, we were able to show that for each of the six events under consideration, CMEs are viable drivers for the metric type II bursts. In each of the six cases, the metric type II began within 1–3 min of the onset of the fast rise in the soft X-ray light curve (flare impulsive phase). Because metric type II bursts characteristically occur within a few minutes of the flare impulsive phase (e.g., Vršnak *et al.*, 1995), our result effectively removes the timing objection (see Cliver and Hudson, 2002) to CMEs as type II drivers.

Support for our conclusion is provided by analysis of Hα, soft X-ray, and EIT data for the six events. In each case, examination of these data for the early

CME launch times inferred from extrapolations of C2 and C3 data (ranging from ~10–60 min before the impulsive phase of the associated flares and the metric type II bursts) revealed no signs of the cataclysmic rearrangement of fields one might expect for a fast CME. Rather we find general evidence in these events (see Table I and Figure 13) for explosive ejecta, wave initiation, and dimming onset near the flare impulsive phase and the accompanying rapid CME acceleration inferred via Zhang *et al.* (2001). The wave associations are pertinent because Biesecker *et al.* (2002) find EIT waves closely associated with CMEs while Klassen *et al.* (2000) find strong association between EIT waves and metric type II bursts (≥90%), consistent with the high degree (93%) of association between CMEs and metric type IIs when coronagraph observing effects are taken into account (N. Gopalswamy, personal communication, 2003). Moreover, West and Thompson (2003) have documented a close relationship between EIT dimmings, taken to represent the source regions of CMEs, and EIT waves. The waves appear at the leading edge of expanding dimming regions (see Figures 4 and 15 for particularly clear examples), consistent with a CME-driver picture at least for the initial phases of the waves (Thompson *et al.*, 2000a). Finally, for two of the six events, including one analyzed by Zhang *et al.* (2001), direct C1 observations support our general conclusion regarding the viability of CME drivers for metric type II bursts.

Our analysis indicates that the CMEs associated with the impulsive flares considered in this study originated in relatively small source regions, with heights of $\sim 10^5$ km and active-region-like angular spans of ~15°, compared with their C2–C3 measured latitudinal spans of >90°. Zhang *et al.* (2004) have recently presented similar evidence for such lateral super-expansion in the low corona for a CME on 11 June 1998 (Raymond *et al.*, 2000).

In Section 3, we discussed key aspects, besides timing, of the debate on the origin of metric type IIs: CME–type II association; connectivity of metric and DH type II bursts; and spatial relationship of CMEs and metric type IIs. Not unexpectedly, the association of CMEs with metric type IIs has increased with the more sensitive LASCO (N. Gopalswamy, personal communication, 2003) versus *Solwind* (Cliver *et al.*, 1999) observations. On the other hand, the apparent discontinuity of many time-associated metric and lower frequency type II bursts (e.g., Leblanc *et al.*, 2000) continues to pose a challenge for the CME-driver scenario, as does radio imaging and spectrographic evidence (e.g., Gary *et al.*, 1984) placing the type II burst behind the CME leading edge. C1 data for the well-observed 6 November 1997 CME (Section 2.8) also indicate that the type II shock formed behind the CME leading edge. Previously, various investigators (e.g., Wagner and MacQueen, 1983; Reiner and Kaiser, 1999) have invoked flare-associated blast waves to interpret such observations, based in part on the close timing relationship between flares and type II bursts. The finding of Zhang *et al.* (2001) that flares and the rapid acceleration phase of CMEs are tightly linked necessitates a new look at the flare-shock explanation for these observations.

5. Discussion

5.1. Ongoing debate: CMEs versus flares

The above summary represents our current brief for the case that metric type II shocks are CME-driven. From the contrary point of view, it can be argued that the proximity of the initiation of the various waves, including the metric type II shock, to the flare impulsive phase (Figure 13) indicates a flare (blast wave or ejecta) origin for the type II bursts. Opting for the blast wave source for these events raises the question of why material moving through the low corona at speeds up to ~2000 km s^{-1} does not drive a coronal shock. We favor a CME-driver over a flare ejecta driver because, in general (Nitta and Akiyama, 1999; see also e.g., Webb and Jackson, 1981), ejecta travels slower than the CME in which it is embedded ("the boat moving slower than the river"; Cliver, 1999), making it an unlikely candidate to drive a shock. In addition, the CME-driver scenario for metric type IIs has the aesthetic value of satisfying Occam's razor because it is generally accepted that DH and lower frequency type IIs are piston-driven by CMEs (e.g., Pick, 1999), particularly when one considers that some fraction of DH type IIs appear to be continuations of metric type IIs, e.g., the 19 May 1998 event in Figure 16 or the two events on 3 November 1997 analyzed by Leblanc *et al.* (2000) and the event on 4 November analyzed by Dulk, Leblanc, and Bougeret (1999). While one cannot rule out multiple origins for metric type II bursts, i.e., blast waves, ejecta, and CMEs giving rise to slow-drift shocks under differing circumstances (e.g., Vršnak, Magdalenić, and Aurass, 2001; Classen and Aurass, 2002), the fact that we have examined six reported exemplars for flare-initiated type II bursts and found instead evidence consistent with a CME-driver scenario strengthens our belief that a fast CME is the "special condition" required for metric type II bursts (Roberts, 1959; Cliver *et al.*, 1999) and that CMEs are the dominant, if not the sole, cause of metric type II radio bursts.

It would be instructive to have well-documented examples during the SOHO/*Yohkoh*/TRACE epoch of metric type II bursts that unambiguously originated in flare blast waves or short-range ejections (see Cliver and Hudson (2002) for a similar comment by Gopalswamy). To the best of our knowledge, none have been reported thus far.

5.2. Emerging consensus: A unified view of energetic wave phenomena

The current widely accepted interpretation of metric type II shocks in terms of active region expansions or short-lived ejecta that drive magnetohydrodynamic (MHD) shocks (e.g., Gopalswamy *et al.*, 1998; Klassen *et al.*, 1999; Leblanc *et al.*, 2000, 2001; Pick, 2001; Vršnak, 2001; Hudson *et al.*, 2003) is based on the pioneering work of Uchida (1960). Subsequently Uchida (1968) turned his attention to Moreton waves (Moreton and Ramsey, 1960) which he modeled as the "sweeping skirt" of

a flare-induced MHD shock wave that propagates upward into the corona. Uchida (1974a,b) presented a unified interpretation of metric type II bursts and Moreton waves. Uchida (1960, 1968) naturally attributed type II bursts and Moreton waves to solar flares ("flare surge" (1960) or flare "flash"/"explosive phase" (1968)) because of the close temporal/spatial association between the waves and flares. At the time, CMEs had not yet been discovered (Koomen *et al.*, 1974).

Recent work by various authors confirms and extends Uchida's (1974a,b) view of the connection between radio shocks and other wave phenomena in the solar atmosphere. Klassen *et al.* (2000) find a high degree of association between type II bursts and EIT waves (Thompson *et al.*, 1998, 1999) and Gopalswamy *et al.* (2000b) presented radio imaging evidence linking a type II burst to an EIT wave (see Harvey, Martin, and Riddle, 1974). Warmuth (2000, 2001, 2004a,b) (see also Thompson *et al.*, 2000a; Pohjolainen *et al.*, 2001) presented evidence that EIT waves and Moreton waves are signatures of the same physical disturbance, viewed at different wavelengths. In a study of 12 events, Warmuth and colleagues conclude that observed speed differences between EIT waves (characteristic speed of several hundred km s^{-1}) and Moreton waves ($\sim$1000 km s^{-1}) resulted from the lower cadence of CME observations and deceleration of the wave. Khan and Aurass (2002) extended the wave unification to those observed in soft X-ray waves (see also Hudson *et al.*, 2003), although agreement on the relationship between the various types of waves is not unanimous with Eto *et al.* (2002), for example, arguing that the EIT and Moreton waves in the 4 November 1997 event are distinct phenomena (cf., Warmuth *et al.*, 2004a).[4]

Thompson *et al.* (2000) speculated that well-defined ("sharp") EIT waves close to the flare site (e.g., Figures 4 and Figure 15) correspond to an early driven phase of the wave, while in the more amorphous waves observed later in an event are freely propagating. The observations of EIT wave deceleration, weakening, and profile broadening by Warmuth *et al.* (2001, 2004a,b) are consistent with this viewpoint. At the same time, observations of type II bursts like that in Figure 16 which exhibit deceleration in the low corona but persist from the metric to the DH range and beyond (Dulk, Leblanc, and Bougeret, 1999; Leblanc *et al.*, 2000) argue for a continuously driven disturbance.

The general movement toward a unified view of flare-associated waves (metric type II shocks, Hα, EIT, soft X-ray, as well as microwave and He I 10830 Å (Warmuth *et al.*, 2004a,b)) has been accompanied by a series of papers referred to above that indicate that a CME rather than a flare is the root cause of these phenomena. The key studies are those by: Biesecker *et al.* (2002) linking EIT waves to CMEs; Zarro *et al.* (1999), Thompson *et al.* (2000b), and Harrison *et al.* (2003) identifying EIT dimmings as the source regions of CMEs; and Thompson *et al.*

[4]Recently, Gilbert and Holzer (2004) reported five separate He 10830 waves in association with a solar event on 25 November 2000. The third and fourth of these waves, occurring close together and originating during the rise of the soft X-ray burst, correspond to the single wave identified in He 10830 for this event by Vršnak *et al.* (2002).

(2000a) and West and Thompson (2003) suggesting an organic relationship between EIT dimmings and waves. With Warmuth *et al.* (2004a,b), we would like to extend Uchida's synthesis of wave flare-associated wave motions in the solar atmosphere to cover the various manifestations that have been observed thus far, although we view them as CME-driven waves rather than as flare-initiated phenomena.

Acknowledgements

We thank Steve Kahler and Dave Webb for comments on the manuscript and acknowledge helpful discussions with Doug Biesecker, Joan Burkepile, Terry Forbes, Nat Gopalswamy, Hugh Hudson, Mike Reiner, Chris St. Cyr (C2/C3 analysis), and Meredith Wills-Davey. We are particularly indebted to Bojan Vršnak for helpful suggestions and constructive criticisms. We thank Henry Aurass and Nigel Prestage for providing spectral radio data from Potsdam and Culgoora, respectively.

References

Alexander, D., Metcalf, T. R., and Nitta, N. V.: 2002, *Geophys. Res. Letters* **29**, 10.1029/2001GL013670.

Bale, S. D., Reiner, M. J., Bougeret, J.-L., Kaiser, M. L., Krucker, S., Larson, D. E., and Lin, R. P.: 1999, *Geophys. Res. Lett.* **26**, 1573.

Biesecker, D. A., Myers, D. C., Thompson, B. J., Hammer, D. M., and Vourlidas, A.: 2002, *Astrophys. J.* **569**, 1009.

Bougeret, J.-L. *et al.*: 1995, *Space Sci. Rev.* **71**, 231.

Brueckner, G. E. *et al.*: 1995, *Solar Phys.* **162**, 357.

Cane, H. V. and Reames, D. V.: 1988, *Astrophys. J.* **325**, 895.

Cane, H. V., Sheeley Jr., N. R., and Howard, R. A.: 1987, *J. Geophys. Res.* **92**, 9869.

Classen, H. T. and Aurass, H.: 2002, *Astron. Astrophys.* **384**, 1098.

Cliver, E. W.: 1999, *J. Geophys. Res.* **104**, 4743.

Cliver, E. W. and Hudson, H. S.: 2002, *J.A.S.T.P.* **64**, 231.

Cliver, E. W., Webb, D. F., and Howard, R. A.: 1999, *Solar Phys.* **187**, 89.

Cliver, E. W. *et al.*: 2001, *Proc. 27th Int. Cosmic Ray Conf.* **8**, p. 3277.

Delaboudinière, J.-P. *et al.*: 1995, *Solar Phys.* **162**, 291.

Delannée, C.: 2000, *Astrophys. J.* **545**, 512.

Delannée, C. and Aulanier, G.: 1999, *Solar Phys.* **190**, 107.

Delannée, C., Delaboudinière, J.-P., and Lamy, P.: 2000, *Astron. Astrophys.* **355**, 725.

Dere, K. P. *et al.*: 1997, *Solar Phys.* **175**, 601.

Dulk, G. A., Leblanc, Y., and Bougeret, J.-L.: 1999, *Geophys. Res. Lett.* **26**, 2331.

Dulk, G. A., McLean, D. J., and Nelson, G. J.: 1985, in D. J. McLean and N. R. Labrum (eds.), *Solar Radiophysics*, Cambridge University Press, New York, NY, p. 53.

Eto, S. *et al.*: 2002, *Pub. Astron. Soc. Japan* **54**, 481.

Gallagher, P. T., Lawrence, G. R., and Dennis, B. R.: 2003, *Astrophys. J. Lett.* **588**, L53.

Gary, D. E. *et al.*: 1984, *Astron. Astrophys.* **134**, 222.

Gergely, T.: 1984, in M. A. Shea, D. F. Smart, and S. M. P. McKenna-Lawlor (eds.), *STIP Symp. Solar/Interplanetary Intervals*, Bookcrafters, Inc., Chelsea, MI, p. 347.

Gergely, T. E. *et al.*: 1984, *Solar Phys.* **90**, 161.

Gilbert, H. R. and Holzer, T. E.: 2004, *Astrophys. J.* **610**, 572.

Giovanelli, R. G. and Roberts, J. A.: 1958, *Australian J. Phys.* **11**, 353.
Gopalswamy, N.: 2000, in R. G. Stone, K. W. Weiler, M. L. Goldstein, and J.-L. Bougeret (eds.), *Radio Astronomy at Long Wavelengths*, Geophys. Mono. 119, AGU, Washington, DC, p. 123.
Gopalswamy, N. and Kaiser, M. L.: 2002, *Adv. Space Res.* **29**, 307.
Gopalswamy, N. and Thompson, B. J.: 2000, *J.A.S.T.P.* **62**, 1457.
Gopalswamy, N., Kundu, M. R., Manoharan, P. K., Raoult, A., Nitta, N., and Zarka, P.: 1997, *Astrophys. J.* **486**, 1036.
Gopalswamy, N. *et al.*: 1998, *J. Geophys. Res.* **103**, 307.
Gopalswamy, N., Nitta, N., Manoharan, P. K., Raoult, A., and Pick, M.: 1999a, *Astron. Astrophys.* **347**, 684.
Gopalswamy, N. *et al.*: 1999b, *J. Geophys. Res.* **104**, 4749.
Gopalswamy, N. *et al.*: 2000a, *Geophys. Res. Lett.* **27**, 1427.
Gopalswamy, N., Kaiser, M. L., Sato, J., and Pick, M.: 2000b, in R. Ramaty and N. Mandzhavidze (eds.), *High Energy Solar Physics – Anticipating HESSI*, ASP Ser. San Francisco, CA, **206**, 351.
Gopalswamy, N., Lara, A., Kaiser, M. L., and Bougeret, M. L.: 2001, *J. Geophys. Res.* **106**, 25261.
Gosling, J. T.: 1993, *J. Geophys. Res.* **98**, 18937.
Gosling, J. T., Hildner, E., MacQueen, R. M., Munro, R. H., Poland, A. I., and Ross, C. L.: 1976, *Solar Phys.* **48**, 389.
Harrison, R. A.: 1995, *Astron. Astrophys.* **304**, 585.
Harrison, R. A., Bryans, P., Simnett, G. M., and Lyons, M.: 2003, *Astron. Astrophys.* **400**, 1071.
Harvey, K. L., Martin, S. F., and Riddle, A. C.: 1974, *Solar Phys.* **36**, 151.
Holman, G. D. and Pesses, M. E.: 1983, *Astrophys. J.* **267**, 837.
Hudson, H. S., Acton, L. W. and Freeland, S. L.: 1996, *Astrophys. J.* **470**, 629.
Hudson, H. S. and Webb, D. F.: 1997, in N. Crooker, J. Joselyn, and J. Feynman (eds.), *Coronal Mass Ejections*, American Geophysical Union, Washington, DC, p. 27.
Hudson, H. S., Khan, J. I., Lemen, J. R., Nitta, N. V., and Uchida, Y.: 2003, *Solar Phys.* **212**, 121.
Hundhausen, A. J.: 1993, *J. Geophys. Res.* **98**, 13177.
Kahler, S. W.: 1993, *Ann. Rev. Astron. Astrophys.* **30**, 113.
Kahler, S. W., Moore, R. L., Kane, S. R., and Zirin, H.: 1988, *Astrophys. J.* **328**, 824.
Kahler, S. W., Sheeley, N. R., Jr., Howard, R. A., Koomen, M. J., and Michels, D. J.: 1984, *Solar Phys.* **93**, 133.
Kaiser, M. L., Reiner, M. J., Gopalswamy, N., Howard, R. A., St. Cyr, O. C., Thompson, B. J., and Bougeret, J.-L.: 1998, *Geophys. Res. Lett.* **25**, 2501.
Kane, S. R.: 1974, in G. Newkirk (ed.), *Coronal Disturbances, Proc.*, IAU Symp. No. 57, D. Reidel, Dordrecht, p. 105.
Karlický, M., Jiřiča, K., Kepka, O., Křivský, L., and Tlamicha, A.: 1982, *Bull. Astron. Inst. Czech.* **33**, 72.
Khan, J. I. and Aurass, H.: 2002, *Astrophys. J.* **383**, 1018.
Khan, J. I. and Hudson, H. S.: 2000, *Geophys. Res. Lett.* **27**, 1083.
Klassen, A., Aurass, H., Klein, K. -L., Hofmann, A., and Mann, G.: 1999, *Astron. Astrophys.* **343**, 287.
Klassen, A. E., Aurass, H., Mann, G., and Thompson, B. J.: 2000, *Astron. Astrophys. Suppl. Ser.* **141**, 357.
Klein, K.-L., Khan, J. I., Vilmer, N., Delouis, J.-M., and Aurass, H.: 1999, *Astron. Astrophys.* **346**, L53.
Koomen, M. J., Howard, R., Hansen, R., and Hansen, S.: 1974, *Solar Phys.* **34**, 447.
Kundu, M. R.: 1965, *Solar Radio Astronomy*, Interscience, New York, NY, p. 362.
Kundu, M. R., White, S. M., Garaimov, V. I., Manoharan, P. K., Subramanian, P., Ananthakrishnan, S., and Janardhan, P.: 2004, *Astrophys. J.* **607**, 530.

Landau, L. D. and Lifshitz, E. M.: 1959, *Fluid Mechanics*, Addison-Wesley, Reading, MA, p. 372ff.
Leblanc, Y., Dulk, G. A., and Bougeret, J.-L.: 1998, *Solar Phys.* **183**, 165.
Leblanc, Y., Dulk, G. A., Vourlidas, A., and Bougeret, J.-L.: 2000, *J. Geophys. Res.* **105**, 18225.
Leblanc, Y., Dulk, G. A., Vourlidas, A., and Bougeret, J.-L.: 2001, *J. Geophys. Res.* **106**, 25301.
Mancuso, S. and Raymond, J. C.: 2004, *Astron. Astrophys.* **413**, 363.
Mancuso, S., Raymond, J. C., Kohl, J., Ko, Y.-K., Uzzo, M., and Wu, R.: 2002, *Astron. Astrophys.* **383**, 267.
Mann, G., Aurass, H., Klassen, A., Estel, C., and Thompson, B. J.: 1999, in J. -C. Vial and B. Kaldeich-Schümann (eds.), *Plasma Dynamics and Diagnostics in the Solar Transition Region and Corona*, ESA SP-446, Noordwijk, p. 477.
Maxwell, A., Dryer, M., and McIntosh, P.: 1985, *Solar Phys.* **97**, 401.
Moreton, G. E. and Ramsey, H. E.: 1960, *Pub. Astron. Soc. Pacific* **72**, 357.
Narukage, N., Hudson, H. S., Morimoto, T., Akiyama, S., Kiyai, R., Kurokawa, H., and Shibata, K.: 2002, *Astrophys. J. Lett.* **572**, L109.
Nelson, G. J. and Melrose, D. B.: 1985, in D. J. McLean and N. R. Labrum (eds.), *Solar Radiophysics*, Cambridge University Press, New York, NY, p. 333.
Neupert, W. M.: 1968, *Astrophys. J.* **153**, L59.
Neupert, W. M., Thompson, B. J., Gurman, J. B., and Plunkett, S. P.: 2001, *J. Geophys. Res.* **106**, 25215.
Newkirk, G.: 1961, *Astrophys. J.* **133**, 983.
Nitta, N. and Akiyama, S.: 1999, *Astrophys. J. Lett.* **525**, L57.
Nitta, N. V. and Hudson, H. S.: 2001, *Geophys. Res. Lett.* **28**, 3801.
Nitta, N., Cliver, E. W., and Tylka, A. J.: 2003, *Astrophys. J. Lett.* **586**, L103.
Ofman, L. and Thompson, B. J.: 2002, *Astrophys. J.* **574**, 440.
Parker, E. N.: 1961, *Astrophys. J.* **133**, 1014.
Pick, M.: 1999, in T. Bastian, N. Gopalswamy, and K. Shibasaki (eds.), *Solar Physics with Radio Observations*, NRO Report No. **479**, Nobeyama, p. 187.
Pohjolainen, S. *et al.*: 2001, *Astrophys. J.* **556**, 421.
Qui, J., Wang, H., Cheng, C. Z., and Gary, D. E.: 2004, *Astrophys. J.* **604**, 900.
Raymond, J. C. *et al.*: 2000, *Geophys. Res. Lett.* **27**, 1439.
Reiner, M. J. and Kaiser, M. L.: 1999, *J. Geophys. Res.* **104**, 16979.
Reiner, M. J., Kaiser, M. L., Plunkett, S. P., Prestage, N. P., and Manning, R.: 2000, *Astrophys. J. Lett.* **529**, L53.
Reiner, M. J., Kaiser, M. L., Gopalswamy, N., Aurass, H., Mann, G., Vourlidas, A., and Maksimovic, M.: 2001, *J. Geophys. Res.* **106**, 25279.
Reiner, M. J. *et al.*: 2003, *Astrophys. J.* **590**, 533.
Roberts, J. A.: 1959, *Australian J. Phys.* **12**, 327.
Robinson, R. D.: 1985, *Solar Phys.* **95**, 343.
Robinson, R. D. and Stewart, R. T.: 1985, *Solar Phys.* **97**, 145.
Rust, D. M.: 1983, *Space Sci. Rev.* **34**, 21.
Saito, K.: 1970, *Ann. Tokyo Astron. Observ.* **12**, 53.
Shanmugaraju, A., Moon, Y.-J., Dryer, M., and Umapathy, S.: 2003, *Solar Phys.* **215**, 185.
Sheeley, N. R., Jr., Stewart, R. T., Robinson, R. D., Howard, R. A., Koomen, M. J., and Michels, D. J.: 1984, *Astrophys. J.* **279**, 839.
St. Cyr, O. C., Burkepile, J. T., Hundhausen, A. J., and Lecinski, A. R.: 1999, *J. Geophys. Res.* **104**, 12493.
Steinolfson, R. S.: 1984, *Solar Phys.* **94**, 193.
Steinolfson, R. S.: 1985, in B. T. Tsurutani and R. G. Stone (eds.), *Collisionless Shocks in the Heliosphere: Reviews of Current Research*, AGU, Washington, DC, p. 1.
Sterling, A. C. and Hudson, H. S.: 1997, *Astrophys. J. Lett.* **491**, 55.

Stewart, R. T.: 1984, *Solar Phys.* **94**, 379.
Subramanian, P. and Dere, K. P.: 2001, *Astrophys. J.* **561**, 372.
Subramanian, P., Ananthakrishnan, S., Janardhan, P., Kundu, M. R., White, S. M., and Garaimov, V. I.: 2003, *Solar Phys.* **218**, 247.
Thompson, B. J., Plunkett, S. P., Gurman, J. B., Newmark, J. S., St. Cyr, O. C., Michels, D. J.: 1998, *Geophys. Res. Lett.* **25**, 2465.
Thompson, B. J. *et al.*: 1999, *Astrophys. J. Lett.* **517**, L151.
Thompson, B. J. *et al.*: 2000a, *Solar Phys.* **193**, 161.
Thompson, B. J., Cliver, E. W., Nitta, N., Delannée, C., and Delaboudinière, J. P.: 2000b, *Geophys. Res. Lett.* **27**, 1431.
Tsuneta, S. *et al.*: 1991, *Solar Phys.* **136**, 37.
Uchida, Y.: 1960, *Pub. Astron. Soc. Japan* **12**, 376.
Uchida, Y.: 1968, *Solar Phys.* **4**, 30.
Uchida, Y., Altschuler, M. D., and Newkirk, G. A.: 1973, *Solar Phys.* **28**, 495.
Uchida, Y.: 1974a, in G. Newkirk (ed.), *Coronal Disturbances*, IAU Symp. **57**, p. 383.
Uchida, Y.: 1974b, *Solar Phys.* **39**, 431.
Vršnak, B.: 2001, *J. Geophys. Res.* **106**, 25291.
Vršnak, B. and Lulić, S.: 2000a, *Solar Phys.* **196**, 157.
Vršnak, B. and Lulić, S.: 2000b, *Solar Phys.* **196**, 181.
Vršnak, B. and Lulić, S.: 2001, *Hvar Observ. Bull.***24**, 17.
Vršnak, B., Magdalenić, J., and Aurass, H.: 2001, *Solar Phys.* **202**, 319.
Vršnak, B., Ruždjak, V., Zlobec, P., and Aurass, H.: 1995, *Solar Phys.* **158**, 331.
Vršnak, B., Warmuth, A., Brajša, R., and Hanslmeier, A.: 2002, *Astron. Astrophys.* **394**, 299.
Vršnak, B., Magdalenić, J., Aurass, H., and Mann, G.: 2002, *Astron. Astrophys.* **396**, 673.
Wagner, W. J. and MacQueen, R. M.: 1983, *Astron. Astrophys.* **120**, 136.
Wang, H., Qui, J., Jing, J., and Zhang, H.: 2003, *Astrophys. J.* **593**, 564.
Warmuth, A.: 2000, Ph.D. Thesis, University of Graz, Oesterreich, Australia.
Warmuth, A., Vršnak, B., Aurass, A., and Hanslmeier, A.: 2001, *Astrophys. J. Lett.* **560**, L105.
Warmuth, A., Vršnak, B., Magdalenić, J., Hanslmeier, A., and Otruba, W.: 2004a, *Astron. Astrophys.* **418**, 1101.
Warmuth, A., Vršnak, B., Magdalenić, J., Hanslmeier, A., and Otruba, W.: 2004b, *Astron. Astrophys.* **418**, 1117.
Webb, D. F. and Howard, R. A.: 1994, *J. Geophys. Res.* **99**, 4201.
Webb, D. F. and Jackson, B. V.: 1981, *Solar Phys.* **73**, 341.
West, M. and Thompson, B. J.: 2003, *Eos, Trans. AGU* 84(46), Fall Meet. Suppl., Abstract SH22B-01.
Wills-Davey, M. J. and Thompson, B. J.: 1999, *Solar Phys.* **190**, 467.
Yurchyshyn, V. B.: 2002, *Astrophys. J.* **576**, 493.
Zarro, D. M., Sterling, A. C., Thompson, B. J., Hudson, H. S., and Nitta, N. V.: 1999, *Astrophys. J. Lett.* **520**, L139.
Zhang, J., Dere, K. P., Howard, R. A., Kundu, M. R., and White, S. M.: 2001, *Astrophys. J.* **559**, 452.
Zhang, J., Dere, K. P., Howard, R. A., and Vourlidas, A.: 2004, *Astrophys. J.* **604**, 420.

REPORT DOCUMENTATION PAGE

Form Approved
OMB No. 0704-0188

1. REPORT DATE *(DD-MM-YYYY)*
17-01-2006

REPRINT

4. TITLE AND SUBTITLE
Coronal Shocks of November 1997 Revisited: The CME-Type II Timing Problem

5a. CONTRACT NUMBER

5b. GRANT NUMBER

5c. PROGRAM ELEMENT NUMBER
61102F

6. AUTHOR(S)
Cliver, E.W., N.V. Nitta*, B.J. Thompson**, and J. Zhang#

5d. PROJECT NUMBER
2311

5e. TASK NUMBER
RD

5f. WORK UNIT NUMBER
A1

7. PERFORMING ORGANIZATION NAME(S) AND ADDRESS(ES)
Air Force Research Laboratory/VSBXS
29 Randolph Road
Hanscom AFB MA 01731-3010

8. PERFORMING ORGANIZATION REPORT NUMBER
AFRL-VS-HA-TR-2006-1012

9. SPONSORING / MONITORING AGENCY NAME(S) AND ADDRESS(ES)

10. SPONSOR/MONITOR'S ACRONYM(S)
AFRL/VSBXS

11. SPONSOR/MONITOR'S REPORT NUMBER(S)

12. DISTRIBUTION / AVAILABILITY STATEMENT
Approved for Public Release; Distribution Unlimited.

*Lockheed Martin Solar & Astro Lab, Palo Alto, CA, **NASA Goddard Space Flt Ctr, Greenbelt, MD, #Ctr for Earth Obseving & Space Res, George Mason Univ, Fairfax, VA

13. SUPPLEMENTARY NOTES
REPRINTED FROM: SOLAR PHYSICS, Vol 225, pp 105-139, 2005.

14. ABSTRACT

Abstract. We re-examine observations bearing on the origin of metric type II bursts for six impulsive solar events in November 1997. Previous analyses of these events indicated that the metric type IIs were due to flares (either blast waves or ejecta). Our point of departure was the study of Zhang *et al.* (2001) based on the Large Angle and Spectrometric Coronagraph's C1 instrument (occulting disk at 1.1 R_0) that identified the rapid acceleration phase of coronal mass ejections (CMEs) with the rise phase of soft X-ray light curves of associated flares. We find that the inferred onset of rapid CME acceleration in each of the six cases occurred 1–3 min before the onset of metric type II emission, in contrast to the results of previous studies for certain of these events that obtained CME launch times ~25–45 min earlier than type II onset. The removal of the CME-metric type II timing discrepancy in these events and, more generally, the identification of the onset of the rapid acceleration phase of CMEs with the flare impulsive phase undercuts a significant argument against CMEs as metric type II shock drivers. In general, the six events exhibited: (1) ample evidence of dynamic behavior [soft X-ray ejecta, extreme ultra-violet imaging telescope (EIT) dimming onsets, and wave initiation (observed variously in Hα, EUV, and soft X-rays)] during the inferred fast acceleration phases of the CMEs, consistent with the cataclysmic disruption of the low solar atmosphere one would expect to be associated with a CME; and (2) an organic relationship between EIT dimmings (generally taken to be source regions of CMEs) and EIT waves (which are highly associated with metric type II bursts) indicative of a CME-driver scenario.

15. SUBJECT TERMS
Type II radio bursts Coronal mass ejections Solar flares

16. SECURITY CLASSIFICATION OF:			17. LIMITATION OF ABSTRACT	18. NUMBER OF PAGES	19a. NAME OF RESPONSIBLE PERSON
a. REPORT		c. THIS PAGE			S. W. Kahler
UNCLAS	UNCLAS	UNCLAS	SAR	10	19b. TELEPHONE NUMBER *(include area code)* 781-377-9665